Li Yan (Orcid ID: 0000-0002-6443-9245)
Chen Xuewei (Orcid ID: 0000-0002-2465-9876)
Xiao Shunyuan (Orcid ID: 0000-0003-1348-4879)
Wu Xianjun (Orcid ID: 0000-0003-0157-0235)
Fan Jing (Orcid ID: 0000-0002-6747-4302)
Wang Wen - Ming (Orcid ID: 0000-0002-6652-5964)

Golovinomyces cichoracearum effector-associated nuclear-localisation of RPW8.2 amplifies its expression to boost immunity in *Arabidopsis*

Jing-Hao Zhao[1], Yan-Yan Huang[1], He Wang[1], Xue-Mei Yang[1], Yan Li[1], Mei Pu[1], Shi-Xin Zhou[1], Ji-Wei Zhang[1], Zhi-Xue Zhao[1], Guo-Bang Li[1], Beenish Hassan[1], Xiao-Hong Hu[1], Xuewei Chen[1], Shunyuan Xiao[2*], Xian-Jun Wu[1*], Jing Fan[1*], Wen-Ming Wang[1*]

[1] State Key Laboratory of Crop Gene Exploration and Utilization in Southwest China and Rice Research Institute, Sichuan Agricultural University, Chengdu, 611131, China

[2] Institute for Bioscience and Biotechnology Research, University of Maryland, College Park, MD 20850, USA

[*] Authors for correspondence:

Wen-Ming Wang e-mail: j316wenmingwang@sicau.edu.cn

Jing Fan e-mail: fanjing13971@sicau.edu.cn

Xian-Jun Wu e-mail: wuxjsau@126.com

Shunyuan Xiao e-mail: xiao@umd.edu

Received: *22 August 2022*

Accepted: *30 November 2022*

Summary

- *Arabidopsis* RESISTANCE TO POWDERY MILDEW 8.2 (RPW8.2) is specifically induced by the powdery mildew (PM) fungus (*Golovinomyces cichoracearum*) in the infected epidermal cells to activate immunity. However, the mechanism of RPW8.2-induction is not well understood.
- Here, we identify a *G. cichoracearum* effector that interacts with RPW8.2, named Gc-RPW8.2 interacting protein 1 (GcR8IP1), by a yeast two-hybrid screen of an *Arabidopsis* cDNA library.
- GcR8IP1 physically associated with RPW8.2 with its RING finger domain that is essential and sufficient for the association. GcR8IP1 was secreted and translocated into the nucleus of host cell infected with PM. Association of GcR8IP1 with RPW8.2 led to an increase of RPW8.2 in the nucleus. In turn, the nucleus-localised RPW8.2 promoted the activity of the *RPW8.2* promoter, resulting in transcriptional self-amplification of *RPW8.2* to boost immunity at infection sites. Additionally, ectopic expression or host-induced gene silencing of *GcR8IP1* supported its role as a virulence factor in PM.
- Altogether, our results reveal a mechanism of RPW8.2-dependent defense strengthening via altered partitioning of RPW8.2 and transcriptional self-amplification triggered by a PM fungal effector, which exemplifies an atypical form of effector-triggered immunity.

Key words : *Arabidopsis thaliana*; broad-spectrum resistance; GcR8IP1; *Golovinomyces cichoracearum*; immunity; nucleocytoplasmic partitioning; powdery mildew; RPW8.2.

Introduction

Plants mount a two-tiered immune system that consists of pattern-triggered immunity (PTI) and effector-triggered immunity (ETI) against microbial pathogens (Jones & Dangl, 2006; Wang *et al.*, 2009). PTI and ETI are mutually potentiated upon their activation by the recognition of the cell-surface and intracellular immune receptors with the conserved pathogen-associated molecular patterns (PAMPs) and pathogen effectors,

respectively (Ngou *et al.*, 2021; Yuan *et al.*, 2021). In many cases, intracellular immune receptors belong to the nucleotide-binding leucine-rich repeat (NLR) proteins that are classified into two broad classes based on their N-terminal domains: Toll and interleukin-1 receptor (TIR) NLRs (TNLs) and coiled-coil (CC) NLRs (CNLs) (Kourelis & Van Der Hoorn, 2018). The TIR domains of TNLs have been demonstrated to possess NADase activity that is mutually exclusive with their 2',3'-cAMP/cGMP synthetase activity, both of which are required for the activation of immune response (Wan *et al.*, 2019; Horsefield *et al.*, 2019; Yu *et al.*, 2022). The CNL ZAR1 resistosome acts as a Ca^{2+}-permeable cation channel in the plasma membrane relaying immune signaling (Wang *et al.*, 2019; Bi *et al.*, 2021). Within CNL proteins, one basal clade is distinguished by having a CC domain resembling the *Arabidopsis thaliana* RESISTANCE TO POWDERY MILDEW 8 (RPW8) proteins, denoted as the CC_R domain (Collier *et al.*, 2011). The CC_R CNLs include two related helper NLRs, namely N-Required Gene 1 (NRG1) and Activated Disease Resistance 1 (ADR1) (Peart *et al.*, 2005; Roberts *et al.*, 2013). In contrast to the CC domain of canonical CNL proteins, the CC_R domains of both NRG1 and ADR1 family proteins are sufficient for the induction of defense responses (Collier *et al.*, 2011). Besides, the ADR1 and NRG1 families play an unequally redundant role in immune signaling transduction of TNL- and CNL-mediated ETI (Dong *et al.*, 2016; Castel *et al.*, 2019; Wu *et al.*, 2019; Saile *et al.*, 2020). These two unique families of NLR proteins have also been termed as RNLs because of their N-terminal CC_R domain homologous to the RPW8 family proteins, which include RPW8.1, RPW8.2, and a few homologues of RPW8 (Xiao *et al.*, 2004; Collier *et al.*, 2011; Dong *et al.*, 2016; Castel *et al.*, 2019). Both RPW8.1 and RPW8.2 confer broad-spectrum resistance to powdery mildew (PM) (Xiao *et al.*, 2001, 2003; Wang *et al.*, 2009; Ma *et al.*, 2014).

PM fungi are obligate biotrophic pathogens that require a living host to complete their lifecycle (Lipka *et al.*, 2008). PM infection induces reorganizations in host cell structure and changes in cell physiology (Hückelhoven & Panstruga, 2011). Particularly, PM fungi establish haustoria in epidermal cells of their hosts to steal water and nutrients

for their proliferation (Lipka *et al.*, 2008). The haustoria of PM are encased by the extra-haustorial membrane (EHM) that forms the host-pathogen interface and the battle frontiers (Kwaaitaal *et al.*, 2017). RPW8.2 is targeted to the EHM via the VAMP721/722-mediated vesicle trafficking pathway upon the invasion of PM fungi that highly induce the expression of *RPW8.2* (Wang *et al.*, 2009; Kim *et al.*, 2014). RPW8.2 is also partitioned into the nucleus and the cytoplasm to mount effective defense responses, such as the deposition of callose to encase the haustorial complex and the enrichment of H_2O_2 in the haustorial complex (Wang *et al.*, 2009; Huang *et al.*, 2019). RPW8.2 engages EDS1-dependent and SA signaling to trigger a positive transcriptional amplification circuit (Xiao *et al.*, 2003, 2005). Intriguingly, *RPW8.2* is strongly and specifically induced in epidermal cells invaded by the adapted PM isolate *Golovinomyces cichoracearum* (*Gc*) UCSC1 (Xiao *et al.*, 2003; Wang *et al.*, 2009). However, it remains unclear how the highly cell-type-specific induction of *RPW8.2* is achieved.

To explore how RPW8.2 activates defense and how RPW8.2 is regulated, we performed a yeast two-hybrid screen and identified a candidate protein from *Gc* USCS1, designated Gc-RPW8.2 interacting protein 1 (GcR8IP1). GcR8IP1 was a secretory protein required for full virulence of *Gc* UCSC1. As a nucleus-localised protein, GcR8IP1 interacted with RPW8.2 and increased RPW8.2's nuclear localisation, leading to a transcriptional self-amplification of *RPW8.2* in haustorium-invaded epidermal cells. Thus, our data provide insight into the mechanism of RPW8.2-mediated immunity against PM as an atypical form of effector-triggered immunity.

Materials and Methods

Plant materials and growth conditions

Arabidopsis thaliana L. accessions Warschau-1 (Wa-1) and Columbia-0 (Col-0) were used in this study. The *pad4-1 sid2-1* double mutant and the transgenic *Arabidopsis* line P2Y3' expressing YFP from the *RPW8.2* promoter were obtained from previous studies (Ma *et al.*, 2014). Seeds were sown directly on soil and vernalized at 4 °C for 2 days

before moving to a growth room at 21 °C and 75% humidity under 10 h/14 h light/dark period. *Nicotiana benthamiana* L. was grown under the same conditions.

Constructs, transient expression, and genetic transformation

For signal peptide verification in yeast, truncated versions of *GcR8IP1* were amplified from *Gc* UCSC1 cDNA and cloned into pSUC2 (Jacobs *et al.*, 1997). For yeast two-hybrid assay, *GcR81IP1* and its truncated versions were amplified from *Gc* UCSC1 cDNA and ligated into pGADT7 (Clontech, USA). For biomolecular fluorescence complementation (BiFC) assay, *GcR81IP1, RPW8.2*, and their mutated/truncated versions were amplified from *Gc* UCSC1 or *Arabidopsis* cDNA and cloned into pJH-YN or pXM-YC. pJH-YN and pXM-YC were derived from BiFC vectors pXY104 and pXY106 by tagging 3×myc and 3×FLAG, respectively (Von Stetten *et al.*, 2012; Luo *et al.*, 2014). For luciferase complementation imaging (LCI) assay, *GcR81IP1, RPW8.2*, and their truncated versions were amplified from *Gc* UCSC1 or *Arabidopsis* cDNA and cloned into pCAMBIA1300-NLuc or pCAMBIA1300-CLuc (Chen *et al.*, 2008). For prokaryotic protein expression, the truncated version *GcR8IP1-M1* was amplified from *Gc* UCSC1 cDNA and cloned into pGEX6p-1 (GE Healthcare, USA). For co-immunoprecipitation (co-IP) and subcellular localisation assays, *GcR8IP1, RPW8.2* and their mutated/truncated versions, tagged with RFP, GFP, 3×FLAG or 3×HA, were separately cloned into pCAMBIA2300 (Leclercq *et al.*, 2010). All primers are listed in Table S1.

For transient expression in *N. benthamiana*, *Agrobacterium tumefaciens* strain GV3101 harbouring individual recombinant plasmid was adjusted to OD_{600} = 0.8 in infiltration buffer (1 mM $MgCl_2$, 10 mM MES pH = 5.7, and 200 μM acetosyringone) before infiltrated into *N. benthamiana* leaves following a previous work (Wydro *et al.*, 2006). For co-expression assays, equal volume of the indicated cultures was mixed thoroughly before infiltration. At 48 h post infiltration, *N. benthamiana* leaves were collected for protein extraction or microscopic observation under a confocal laser scanning microscope (Nikon A1, Japan).

For silencing *GcR8IP1* via the host-induced gene silencing (HIGS) technique, the *GcR8IP1* fragment spanning from 27-bp to 382-bp, covering the RING domain-encoding sequence, was amplified and cloned into pHB through an intermediate vector pKANNIBAL (Varsha Wesley *et al.*, 2001). The *GFP* fragment spanning from 62-bp to 462-bp was cloned into pHB as a negative control. To overexpress *GcR8IP1* in *Arabidopsis*, full length of *GcR8IP1* tagged with *3×HA* was clone into pER8 to generate XVE-GcR8IP1-HA-OE expression cascade (Schlücking *et al.*, 2013). All primers are listed in Table S1. The floral dip method was used for *Arabidopsis* transformation as described (Clough & Bent, 1998). Transgenic plants were selected in soil by spraying with 15 mg/L Basta.

Yeast two-hybrid assay

Yeast two-hybrid (Y2H) assays were performed according to the manufacturer's protocol (Clontech, USA). For Y2H screening, the full length of *RPW8.2* coding sequence was cloned into the pGBKT7 as a bait, which was used for screening against an *Arabidopsis* cDNA library conditioned with *Gc* UCSC1 infection.

For detecting protein interaction, BD-RPW8.2-NT or BD-RPW8.2-CT was co-transformed with AD-GcR8IP1-M1, AD-GcR8IP1-M2, or AD-RING into yeast strain Y2HGold (Clontech, USA). Positive clones were stripped onto DDO (SD/-Trp/-Leu) or QDO (SD/-Leu/-Trp/-Ade/-His) medium and incubated at 30 °C for 3 days.

Protein expression and purification from *Escherichia coli*

The pGEX6p-1-GcR8IP1-M1 construct was transformed into *E. coli* strain Rosetta™ (DE3) (Sigma-Aldrich, USA). The resultant was cultured in liquid Luria-Bertani medium supplied with 20 mM Isopropyl β-D-1-Thiogalactopyranoside for expression of recombinant proteins. Recombinant proteins were purified using glutathione resin according to the manufacturer's instructions (GE healthcare, USA).

Semi *in vitro* protein–protein interaction assay

The *in vitro* protein-protein interaction assay was performed as described with

modifications (Chang *et al.*, 2013). Briefly, 1 mg of purified GST or GST-GcR8IP1-M1 fusion protein was incubated with 50 μL glutathione resin at 4 °C for 4 h, washed with buffer A (150 mM NaCl, 50 mM Tris-Cl, pH 7.4, 0.1% Tween 20, protease inhibitor cocktail, and 1mM DTT) for eight times (each time 5 min), and then incubated for 2 h with 5 mL protein isolated from 2.0 g *N. benthamiana* leaves-expressing the RPW8.2-HA construct. After incubation, the resin was collected, washed with buffer A for six times, resuspended in 4 × SDS sample buffer, and boiled for 5 min. The resulting proteins were detected by Western blot analysis with GST and HA antibodies (Cell Signaling Technology, USA).

Co-immunoprecipitation assay

For co-IP assay, RPW8.2-FLAG was co-expressed with GcR8IP1-HA or GcR8IP1-M2-HA in *N. benthamiana*. Total protein was extracted with extraction buffer (50 mM HEPES, pH 7.5, 150 mM KCl, 1 mM EDTA, 0.5% Triton X-100, 1 mM DTT, and 1× proteinase inhibitor cocktail). For IP, total protein was incubated with 50 μL agarose-conjugated HA antibody for 4 h, washed with the extraction buffer for eight times, eluted with 0.5 mg/mL 3× HA peptide for 0.5 h, and then subjected to Western blotting with HA and FLAG antibodies (Cell Signaling Technology, USA). Isolation of cytoplasmic and nuclear protein was performed as described previously (Wang *et al.*, 2011). The resulting proteins were detected by Western blot analysis with R8IP1, HA, H3 (Sigma-Aldrich, USA), and PEPC (Abcam, UK) antibodies. The R8IP1 antibody was raised in rabbits with a recombinant peptide including 207-352 aa of GcR8IP1 (HuaBio, China).

Luciferase complementation imaging assay

For luciferase complementation imaging (LCI) assay, *N. benthamiana* leaves were co-infiltrated with the agrobacteria carrying the NLuc and CLuc derivative constructs. The infiltrated leaves were sprayed with 1 mM luciferin at 48 h after infiltration and examined under a cooled charge coupled device imaging apparatus (Bio-Rad

ChemiDoc XRS+, USA). Luciferase activity was quantified by a GloMax96 luminometer (Promega, USA).

Validation of signal peptide

To verify the functionality of GcR8IP1 signal peptide, plasmids of pSUC2-GcR8IP1^{16aa}, pSUC2-GcR8IP1^{26aa}, pSUC2-GcR8IP1^{40aa}, pSUC2-Avr1b^{SP}, and pSUC2-Mg87^{N} were separately transformed into yeast strain YTK12 and subjected to yeast secretion assay as performed previously (Li *et al.*, 2021). To further confirm the functionality of GcR8IP1^{40aa} in secretion, GcR8IP1^{40aa}-GFP was transiently expressed in *N. benthamiana* leaves and treated with/without 12% (m/v) sucrose solution for 10 min, prior to observation under a confocal laser scanning microscope (Nikon A1, Japan).

Immunofluorescence assay

At 3 days post inoculation (dpi), healthy or *Gc* UCSC1-infected *Arabidopsis* leaves were fixed with 4% paraformaldehyde and embedded with paraffin. Semi-thin (6-8 μm) sections were prepared and immersed in blocking buffer (10% normal goat serum in PBS-T) for 30 min, and then incubated for 4 h in 1% normal goat serum in PBS-T that contains the R8IP1 antibody (1: 300 dilution). After washing with PBS-T for three times (5 min for each washing), an Alexa Fluro 488-conjugated secondary antibody (1: 600 dilution) was used to detect the *in situ* localisation of GcR8IP1 under a confocal laser scanning microscope (Nikon A1, Japan). 4',6-diamidino-2-phenylindole (DAPI) was used to stain the nucleus.

Measurement of the maximum photochemical efficiency of PSII

Eight-week-old *Arabidopsis* plants were challenged with *Gc* UCSC1 and measured for potential quantum efficiency of PSII at 10 dpi by calculating the ratio Fv/Fm [(Fm–Fo)/Fm] on a Chlorophyll Fluorescence Imager (Technologica, UK) (Butler & Kitajima, 1975).

Diaminobenzidine staining assay

Leaves were stained for H_2O_2 *in situ* using the 3,3'-diaminobenzidine (DAB) technique.

Briefly, leaves were immersed in 1 mg/mL DAB solution (0.2 M sodium phosphate buffer, pH 7.0) overnight in dark and destained by 95% ethanol, prior to image capture under a Zeiss Axio Imager A2 (Zeiss, Germany).

Measurement of reactive oxygen species and callose deposition

Reactive oxygen species (ROS) was measured as described (Li *et al.*, 2010). Briefly, 3-mm leaf discs were prepared and floated on ddH_2O for 8 h. ddH_2O was carefully removed before adding 200 mL buffer containing 100 µg/mL chitin, 20 mM luminol, and 1 mg horseradish peroxidase. Luminescence was recorded with a GloMax96 luminometer (Promega, USA). Callose deposition in *Arabidopsis* leaves was examined as described previously (Mason *et al.*, 2020). Aniline blue staining was conducted as reported (Brundrett *et al.*, 1988).

Reverse transcription-PCR and Real-Time PCR

Total RNA was extracted from *Arabidopsis* leaves using the TRIzol Reagent (Invitrogen) and then treated with RNase-free DNase I (Takara) to remove the potential DNA contamination. The first-strand cDNA was synthesized from 1 µg of total RNA. For fungal biomass analysis, total DNA was isolated from the PM infected leaves. The relative quantity of *G. cichoracearum* DC. *GDSL*-like lipase gene in *Gc* UCSC1 was normalized to the *Arabidopsis GAPCP-2* (*At1g16300*) to calculate the fungal biomass of PM in infected leaves (Weßling & Panstruga, 2012). The primers used for RT-PCR and Real-Time PCR are listed in Table S1.

Results

RPW8.2 interacts with a powdery mildew protein GcR8IP1

In a yeast two-hybrid screen against a cDNA library derived from PM-infected *Arabidopsis* leaves, we identified a candidate RPW8.2-interacting protein (R8IP) encoded by *G. cichoracearum*, designated as GcR8IP1 (GenBank accession no.: MH404184). GcR8IP1 possesses 352 amino acids (aa), containing a REALLY INTERESTING NEW GENE (RING) domain and a MENAGE A TROIS 1 (MAT1)

domain (Fig. 1a). The first 129-aa of GcR8IP1 (hereafter GcR8IP1-M1) that was screened out by Y2H contains the RING domain and partial of the MAT1 domain. GcR8IP1 is highly conserved among different PM fungi, especially at the RING domain (Fig. S1).

RPW8.2 is divided into N terminus (NT, the first 100 aa) including two nuclear localisation signals (NLSs) and C terminus (CT, 101-174 aa) including two nuclear export signals (NESs) (Fig. 1a) (Huang *et al.*, 2014, 2019). Both RPW8.2-NT and RPW8.2-CT interacted with GcR8IP1-M1 and the RING domain (18-61 aa), but not with the RING-deleted mutant (M2) of GcR8IP1 in yeast (Fig. 1b). Protein expression was confirmed by Western blot analysis (Fig. S2a). BiFC assays showed that RPW8.2 was associated with GcR8IP1 in the nucleus, and the RING domain of GcR8IP1 was sufficient for the interactions with RPW8.2-NT and RPW8.2-CT (Fig. 1c and Fig. S2b). Intriguingly, RPW8.2 and GcR8IP1-M1 were co-localised in the nucleus as puncta (Fig. S2c). The interaction between RPW8.2 and GcR8IP1 was further confirmed by GST pull-down, co-IP, and LCI assays (Fig. 1d and Fig. S2d, 2e).

GcR8IP1 is secreted and translocated into host nucleus during PM infection

We next examined whether *GcR8IP1* is expressed during PM infection in *Arabidopsis* and found that the expression of *GcR8IP1* was up-regulated at 3 days post inoculation (dpi), 4 dpi, and 6 dpi of *Gc* UCSC1 in rosette leaves of *Arabidopsis* (Fig. S3a). The fungal biomass maintained at a low amount and showed no significant difference within 6 dpi, but had a sharp increase at 7 dpi and 12-13 dpi (Fig. S3b). It is well-known that the establishment of haustoria starts at 24 hours post inoculation and reaches a summit at 3-4 dpi, events that support the proliferation and sporulation of PM at 5-6 dpi (Koh *et al.*, 2005; Micali *et al.*, 2008). Therefore, the expression pattern of *GcR8IP1* may be associated with the establishment of the haustoria and sporulation of PM.

To verify whether GsR8IP1 could be translocated into host cells during PM infection, we first tested whether GcR8IP1 could be secreted. Although SignalP 6.0 predicted no signal peptide in GcR8IP1, SecretomeP 2.0 predicted that GcR8IP1 was a putative

secretory protein with a NN score (neural network output score) of 0.774, which is above a threshold of 0.6 (Bendtsen *et al.*, 2004; Teufel *et al.*, 2022). We next determined which peptide might lead to the secretion of GcR8IP1 by using a yeast secretion assay as described previously (Jacobs *et al.*, 1997). We found that the first 16, 26, and 40 aa at the N-terminus of GcR8IP1 enabled the invertase secretion-deficient mutant YTK12 to grow on the YPRAA medium and to transform TTC (2,3,5-triphenyl-2-tetrazolium chloride) into red insoluble substance, indicating that these peptides drove the secretion of invertase in yeast (Fig. 2a). Consistently, the first 40 aa of GcR8IP1 fused with GFP was detected in the apoplast space when transiently expressed in leaf epidermal cells of *N. benthamiana*, indicating secretion *in planta* (Fig. 2b). These results indicate that GcR8IP1 is a secretory protein containing an unconventional signal peptide.

We then made a polyclonal antibody for GcR8IP1 and used immunofluorescence assay to examine its subcellular localisation during PM infection. Whereas the mock treatment generated a background signal, more intense signals were observed in the nuclei of both the haustorium and the host cell as puncta than in the other organelles (Fig. 2c), indicating that GcR8IP1 is delivered into the host cell and localised in the nucleus. Transient expression in *N. benthamiana* showed that GcR8IP1-RFP (with/without the peptide directing secretion) was localised in the nucleus (Fig. S4). These data indicate that GcR8IP1 is secreted and could be translocated into host nucleus through an unknown mechanism.

Expression of GcR8IP1 increases the amount of nucleus-localised RPW8.2

To investigate the biological impact of GcR8IP1's interaction with RPW8.2, we conducted a series of co-expression assays following a previous report (Huang *et al.*, 2014). RPW8.2-GFP was localised mainly in the cytoplasm and rarely in the nucleus when *R82$_{pro}$:RPW8.2-GFP* was co-expressed with *35S$_{pro}$:2RFP-NLS* (Fig. 3a). Intriguingly, RPW8.2-GFP was obviously detected in the nucleus when *R82$_{pro}$:RPW8.2-GFP* was co-expressed with *35S$_{pro}$:GcR8IP1-RFP* (Fig. 3a, Fig. S5**)**. The percentage of nuclei with RPW8.2-GFP signal was remarkably higher in the leaf epidermal cells co-expressing *R82$_{pro}$:RPW8.2-GFP* with *35S$_{pro}$:GcR8IP1-RFP* than

those co-expressing *R82$_{pro}$:RPW8.2-GFP* with *35S$_{pro}$:2RFP-NLS* (Fig. 3b). Consistently, RPW8.2-GFP was highly co-localised with GcR8IP1-RFP in the nucleus (Fig. 3c-f). These data indicate that GcR8IP1's interaction with RPW8.2 alters the nucleocytoplasmic partitioning of RPW8.2 and increases its nuclear localisation.

Next, we prepared the cytoplasmic and nuclear fractions from total proteins extracted from the *N. benthamiana* leaves co-expressing *35S$_{pro}$:RPW8.2-HA* with *35S$_{pro}$:2RFP-NLS* or *35S$_{pro}$:GcR8IP1* and examined the abundance of RPW8.2-HA by immunoblot analysis with two internal references for the fractionation procedure, namely a cytosolic protein marker (phosphoenolpyruvate carboxylase [PEPC]) and a nuclear protein marker (histone H3). PEPC was detected only in the cytoplasmic fractions and histone H3 only in the nuclear fractions, indicating minimal contamination between the cytoplasmic and nuclear fractions (Fig. 3g). Consistent with the subcellular localisation, RPW8.2-HA was detected mainly in the cytoplasmic fractions but barely in the nuclear fractions when *35S$_{pro}$:RPW8.2-HA* was co-expressed with *35S$_{pro}$:2RFP-NLS*. In contrast, RPW8.2-HA was detected in both the cytoplasmic and the nuclear fractions when *35S$_{pro}$:RPW8.2-HA* was co-expressed with *35S$_{pro}$:GcR8IP1* (Fig. 3g), indicating that GcR8IP1 alters the nucleocytoplasmic partitioning of RPW8.2.

We then investigated whether the NLS of GcR8IP1 is required for altering nucleocytoplasmic partitioning of RPW8.2. We observed that the percentage of nuclei with RPW8.2-GFP was remarkably reduced when *35S$_{pro}$:RPW8.2-GFP* was co-expressed with *35S$_{pro}$:GcR8IP1^{nls}-RFP* in which the NLS of GcR8IP1 was mutated. By contrast, when the NLS of RPW8.2 was mutated, the RPW8.2^{nls}-GFP protein was still recruited by GcR8IP1-RFP into nuclei (Fig. 3h, i). These data indicate that GcR8IP1-associated nuclear localisation of RPW8.2 is dependent on the NLS of GcR8IP1, but not the NLS of RPW8.2.

Nucleus-localised RPW8.2 promotes the activity of the *RPW8.2* promoter

RPW8.2 is induced by PM infection presumably via SA-dependent feedback amplification (Xiao *et al.*, 2003; Wang *et al.*, 2009). To test whether the nucleus-

localised RPW8.2 is crucial for such a feedback amplification, we measured the expression of a firefly luciferase (LUC) reporter under the control of the *RPW8.2* promoter (*R82$_{pro}$:LUC*) when it was separately co-expressed with a wild type RPW8.2 (*35S$_{pro}$:RPW8.2*), a NLS-fused RPW8.2 (*35S$_{pro}$:RPW8.2-HA-NLS$_{Sv40}$*), a NES-fused RPW8.2 (*35S$_{pro}$:RPW8.2-HA-NES$_{PKI}$*) (Huang *et al.*, 2014), or a mutated NLS-fused RPW8.2 (*35S$_{pro}$:RPW8.2-HA-nls$_{Sv40}$*) (Huang *et al.*, 2019). The activity of *R82$_{pro}$:LUC* was enhanced when it was co-expressed with *35S$_{pro}$:RPW8.2-HA-NLS$_{Sv40}$*, but suppressed when co-expressed with *35S$_{pro}$:RPW8.2-HA-NES$_{PKI}$*, compared with the co-expression with the empty vector (EV), the wild-type control, and *35S$_{pro}$:RPW8.2-HA-nls$_{Sv40}$* (Fig. 4a), implying that nucleus-localised RPW8.2 increases the activity of the *RPW8.2* promoter.

To evaluate the effect of the interaction between RPW8.2 and GcR8IP1 on the *RPW8.2* promoter activity, we examined the amount of RPW8.2-YFP expressed from the *RPW8.2* promoter (*R82$_{pro}$:R82Y*) when it was co-expressed with RPW8.2-HA (*35S$_{pro}$:R82HA*), or with RPW8.2-HA plus GcR8IP1 (*35S$_{pro}$:GcR8IP1*) in *N. benthamiana*. The RPW8.2-YFP signal from *R82$_{pro}$:R82Y* was obviously more intense when *R82$_{pro}$:R82Y* was co-expressed with *35Spro:RPW8.2-HA* plus *35S$_{pro}$:GcR8IP1* than co-expressed with *35S$_{pro}$:R82HA* (Fig. 4b). Immune blotting analysis confirmed that more RPW8.2-YFP accumulated when *R82pro:R82Y* was co-expressed with *35S$_{pro}$:R82HA* plus *35S$_{pro}$:GcR8IP1* than co-expressed with *35S$_{pro}$:R82HA* (Fig. 4c), indicating that the co-expression of GcR8IP1 may enhance the transcription of *R82$_{pro}$:R82Y* or stabilize RPW8.2-YFP, or both. Compared with GcR8IP1, the GcR8IP1-M1 (including the RING and partial MAT1 domains) and GcR8IP1^{MAT1} truncations failed to increase the accumulation of RPW8.2 (Fig. S6). Moreover, the activity of *R82$_{pro}$:LUC* was significantly increased in its co-expression with *35S$_{pro}$:RPW8.2* plus *35S$_{pro}$:GcR8IP1* than its co-expression with *35S$_{pro}$:RPW8.2* or *35S$_{pro}$:GcR8IP1* (Fig. 4d), indicating that co-expression of GcR8IP1 and RPW8.2 enhances the *RPW8.2* promoter activity presumably due to the increase of the partitioning of RPW8.2 in the nucleus.

To test whether GcR8IP1 also stabilizes RPW8.2, we examined the accumulation of RPW8.2-YFP from co-expression of *35S$_{pro}$:RPW8.2-YFP* with *35S$_{pro}$:GcR8IP1*, *35S$_{pro}$:RPW8.2-HA-NLS*, *35S$_{pro}$:RPW8.2-HA-NES$_{PKI}$*, or *35S$_{pro}$:RPW8.2-HA*. Again, the most abundant accumulation of RPW8.2-YFP was detected when *35S$_{pro}$:RPW8.2-YFP* was co-expressed with *35S$_{pro}$:GcR8IP1*, followed sequentially by co-expression with *35S$_{pro}$:RPW8.2-HA-NLS*, *35S$_{pro}$:RPW8.2-HA*, and *35S$_{pro}$:RPW8.2-HA-NES$_{PKI}$* (Fig. 4e), indicating that GcR8IP1 may also prevent RPW8.2 from degradation.

RPW8.2 and GcR8IP1 are engaged in a molecular warfare at the infection sites

To test whether GcR8IP1 triggers RPW8.2-mediated immunity against PM as the current concept of ETI, we first examined ROS production induced by the expression of RPW8.2 in *N. benthamiana*. To our surprise, ROS production was significantly suppressed when *35S$_{pro}$:RPW8.2* was co-expressed with *35S$_{pro}$:GcR8IP1* (Fig. S7a). Transient expression of the RPW8.2 C-terminal (CC$_{RPW8.2,}$ 101-174 aa of RPW8.2) triggers cell death in *N. benthamiana* (Huang *et al.*, 2019), which was delayed by GcR8IP1 (Fig. S7b). These data indicate GcR8IP1 may suppress RPW8.2-mediated immunity.

We then tested the effect of GcR8IP1 on RPW8.2-mediated immunity in *Arabidopsis*. We intended to construct transgenic *Arabidopsis* plants expressing *35S$_{pro}$:GcR8IP1-GFP*, *35S$_{pro}$:RFP-GcR8IP1* or *35S$_{pro}$:GcR8IP1-RFP*. Unfortunately, we failed to detect GFP or RFP signals or proteins in the transgenic lines, although we detected the transcripts of *GcR8IP1-RFP* (Fig. S8a, b). Then, we used the XVE expression cassette to make the β-estradiol inducible expression of *GcR8IP1-HA* (XVE-*GcR8IP1-HA*-OE) in *Arabidopsis* accession Col-0 that lacks *RPW8.1* and *RPW8.2* and Wa-1 that contains *RPW8.1* and *RPW8.2* following a previous report (Orgil *et al.*, 2007; Schlücking *et al.*, 2013). GcR8IP1-HA was detected at 6, 12, and 24 hours after β-estradiol treatment and peaked at 12 hours in the transgenic lines in both Col-0 and Wa-1 backgrounds (Fig. S8c, d). These observations imply that GcR8IP1 only transiently accumulates when heterologously expressed in *Arabidopsis*.

We next used the transgenic lines with β-estradiol inducible expression of GcR8IP1-HA in Wa-1 background (Wa-1/XVE-*GcR8IP1-HA*-OE). The infection of PM leads to a decrease in photochemical efficiency that can be measured as chlorophyll fluorescence parameter Fv/Fm in the infected leaves (Kuckenberg *et al.*, 2009). Photochemical efficiency assay showed that relative chlorophyll fluorescence (Fv/Fm) was decreased in β-estradiol treated Wa-1/XVE-*GcR8IP1-HA*-OE lines, indicating more PM fungal growth on the GcR8IP1-expressing leaves (Fig. 5a, b). Consistently, the β-estradiol-treated Wa-1/XVE-*GcR8IP1-HA*-OE plants accumulated less H_2O_2 and supported significantly more fungal biomass than mock-treated plants (Fig. 5c and Fig. S10a, b). Nevertheless, the β-estradiol-treated Wa-1/XVE-*GcR8IP1-HA*-OE plants accommodated comparable numbers of conidiospores as the control plants, indicating effective resistance as supported by the disease resistance phenotypes (Fig. 5d and Fig. S9). This is in consistence with the finding that the expression of defense marker genes was induced in β-estradiol-treated Wa-1/XVE-*GcR8IP1-HA*-OE plants to comparable levels as in control plants at 48 hpi (Fig. S10c, d).

The transcription of *RPW8* was positively regulated via an SA-dependent feedback loop and *RPW8.2* expression continually increased from 1 dpi with *Gc* UCSC1 and remained at high abundance at 7 dpi (Xiao *et al.*, 2003, 2005). Consistently, the expression of *RPW8.2-YFP* from the *RPW8.2* promoter was highly up-regulated at 24 h, reaching approximately 1269 times higher than that at 0 h upon the treatment of the SA-functional analogue benzo (1,2,3) thiadiazole-7-carbothioic acid (BTH) (Fig. S11a). Surprisingly, the accumulation of RPW8.2-YFP protein was still undetectable at this time point (Fig. S11b), indicating that RPW8.2 in uninfected cells (in the absence of GcR8IP1) is constantly removed, which is consistent with our earlier report that RPW8.2 is turned over via both the 26S proteasome and the vacuole-dependent pathway in the cytoplasm (Huang *et al.*, 2019). However, in transgenic *Arabidopsis* plants expressing YFP from the *RPW8.2* promoter, strong YFP expression was detected in haustorium-infected epidermal cells, but weak YFP signal was occasionally observed in adjacent cells (Fig. 5e) (Ma *et al.*, 2014). These data imply that RPW8.2 in

haustorium-invaded cells undergo a rapid and strong self-amplification, while RPW8.2 in uninfected cells is rapidly removed via the 26S proteasome and vacuole-dependent degradation. Hence, GcR8IP1 plays a role in inducing RPW8.2 expression and inhibiting RPW8.2's degradation, leading to a strong and sustained up-regulation of RPW8.2 at the infection sites.

GcR8IP1 is a virulence factor facilitating powdery mildew pathogenesis

To determine the role of *GcR8IP1* in PM pathogenesis, we inoculated the Col-0/XVE-*GcR8IP1-HA*-OE lines (Fig. S8a) with *Gc* UCSC1 after β-estradiol or mock treatment. Compared with the mock treatment, β-estradiol-treated plants exhibited enhanced susceptibility to PM, indicated by decreased photochemical efficiency (Fig. 6a, b). More conidiospores and fungal biomass were generated on β-estradiol-treated Col-0/XVE-*GcR8IP1-HA*-OE lines than those on Col-0 and mock-treated lines (Fig. 6c, d). Less H_2O_2 accumulation and defense gene induction were detected in the β-estradiol-treated Col-0/XVE-*GcR8IP1-HA*-OE plants than those in controls (Fig. S12a-d). These results indicate that ectopic expression of *GcR8IP1* results in enhanced susceptibility to PM in *Arabidopsis*, which is likely attributed to that GcR8IP1 suppressed chitin-triggered immune responses, such as ROS production and callose deposition (Fig. S12e-g).

We further confirmed the virulence role of *GcR8IP1* in PM pathogenesis by a host-induced gene silencing (HIGS) approach (Nowara *et al.*, 2010). We made *R8IP1-IR* and *GFP-IR* transgenic plants in the background of *pad4-1 sid2-1* mutant, which is highly susceptible to *Gc* UCSC1 and facilitates disease phenotyping (Fig. S13). Upon inoculation of *Gc* UCSC1 at 6 dpi, the expression of *GcR8IP1* was significantly down-regulated in the *R8IP1-IR* lines but not in the *GFP-IR* lines (Fig. 6e), indicating effective HIGS of *GcR8IP1*. Disease assay indicated that *R8IP1-IR* lines exhibited less proliferation of PM than the wild-type and *GFP-IR* lines at 6 dpi (Fig. 6f). Consistently, conidiospore production was significantly decreased in *R8IP1-IR* lines in comparison with the wild-type and *GFP-IR* lines (Fig. 6g). These results indicate that HIGS of *GcR8IP1* reduced *Gc* UCSC1 virulence in *pad4-1 sid2-1*. Thus, *GcR8IP1* is required

for the full virulence of *Gc* UCSC1.

Discussion

During canonical ETI, plant NLR receptors detect their cognate effectors, i.e., avirulence (Avr) factors to initiate defense responses summited by the hypersensitive response (HR) (Jones & Dangl, 2006). Here, we found that the PM effector GcR8IP1 acts like an Avr that activates RPW8.2. GcR8IP1 physically associates with RPW8.2 to increases its partitioning into the nucleus, which in turn, amplifies *RPW8.2* expression to boost immunity (Fig. 7).

GcR8IP1 is a secreted effector delivered into the nuclei of host cells (Fig. 2c). Even though no canonical SP was predicted at the N-terminus of GcR8IP1 by online prediction software, the first 16 to 40 aa drove secretion of a reporter peptide in yeast or *in planta* (Fig. 2a, b), indicating an unconventional SP different from the five reported types of SPs (Teufel *et al.*, 2022). Moreover, immunolocalisation assays demonstrated that GcR8IP1 formed puncta in the nucleus of haustorium-invaded epidermal cells of *Arabidopsis* plants upon inoculation of *Gc* UCSC1. Such GcR8IP1-positive puncta are similar to those detected in BiFC that indicates direct interaction between GcR8IP1 and RPW8.2 (Fig. 2c and Fig. S2c). These data indicate that GcR8IP1 is secreted by *Gc* UCSC1 and delivered into host cells and imply that its interaction with RPW8.2 or homologs in *Arabidopsis* may be attributable to GcR8IP1's puncta localisation in the nucleus.

PM infection remarkably induces the expression of RPW8.2, which is partitioned to the EHM, the nucleus and the cytoplasm (Wang *et al.*, 2009; Huang *et al.*, 2019). The EHM-targeting of RPW8.2 is obviously induced upon the establishment of the haustorial complex. Here, we found that PM infection also impacted the partitioning of RPW8.2 into the nucleus via its association with GcR8IP1. Apparently, when GcR8IP1 is delivered to the nucleus of the host cell upon PM infection, its association with RPW8.2 facilitates the nuclear localisation of RPW8.2, thus increasing the partitioning of RPW8.2 in the nucleus (Fig. 3). Because RPW8.2 is known to engage an SA-

signaling–dependent transcriptional self-amplification circuit (Xiao *et al.*, 2003, 2005), increased nucleus-localised RPW8.2 further activates the *RPW8.2* promoter, leading to a rapid transcriptional self-amplification (Fig. 4 and Fig. 5e). Thus, the combinatorial impacts of GcR8IP1 on *RPW8.2*'s expression and accumulation provide a detailed mechanistic explanation as to why RPW8.2 is highly and specifically induced and functions in haustorium-invaded cells upon PM infection (Fig. 7).

GcR8IP1 possesses a RING finger domain and a MAT1 domain that are present in MAT1/Tfb3 (RNA polymerase II transcription factor B subunit 3) protein family members. MAT1/Tfb3 acts as an assembly factor for cyclin-dependent kinase-activating kinase (CAK) enzymatic complex and DNA repair factor IIH (TFIIH), playing roles in general gene transcription and DNA repair (Feaver *et al.*, 1997; Schultz *et al.*, 2000). The RING finger domain of MAT1/Tfb3 protein is crucial for transcription activation (Busso *et al.*, 2000). Here, we demonstrated that the RING of GcR8IP1 was required for its association with RPW8.2 and thus for re-localisation of RPW8.2 to the nucleus (Fig. 1 and Fig. 3). GcR8IP1 likely targets other unidentified host targets for inhibiting host immune responses and facilitating PM infection in *Arabidopsis* lacking *RPW8.2* (Fig. 6 and Fig. S12). However, the virulence targets of GcR8IP1 and the underlying mechanisms need to be clarified in future work. Together, GcR8IP1 is a type of pathogen effector that affects plant gene transcription.

Re-localisation of plant targets is an important mechanism for pathogen effectors to manipulate host immunity and metabolism. *Phytophthora sojae* effector PsAvh52 targets a soybean transacetylase GmTAP1 and causes re-localisation of GmTAP1 from cytoplasm into the nucleus to acetylate histones H2A and H3, thus increasing susceptibility to *P. sojae* (Li *et al.*, 2018). *Ustilago maydis* effector Rip1 binds with and re-localises the maize lipoxygenase 3 (Zmlox3) from cytosol to the nucleus for suppressing host ROS burst (Saado *et al.*, 2022). *Ustilaginoidea virens* effector UvSec117 interacts with and recruits the rice deacetylase OsHDA701 to the nucleus to reduce histone H3K9 acetylation levels, resulting in attenuation of defense gene activation and disease resistance (Chen *et al.*, 2022). Interestingly, re-localisation of

host proteins by effectors may also lead to plant resistance. For instance, *Ralstonia solanacearum* PopP2 effector triggers the re-localisation of an *Arabidopsis* cysteine protease RD19 to the nucleus, leading to RRS1-R-mediated resistance (Bernoux *et al.*, 2008). Similarly, we found that GcR8IP1 promoted accumulation of RPW8.2 in the nucleus, leading to enhanced defense against PM (Fig. 4) (Huang *et al.*, 2019). It should be noted that overexpression of *GcR8IP1* facilitated PM mycelial growth even in the presence of *RPW8.2* (in Wa-1), although the PM sporulation was constrained (Fig. 5c, d). This might be due to that GcR8IP1 re-localised RPW8.2 from cytoplasm to nucleus to delay RPW8.2-mediated cell death (Fig. S7), since cytoplasm-localised RPW8.2 is responsible for inducing cell death (Huang *et al.*, 2019).

GcR8IP1, particularly its RING finger domain, is highly conserved among tested powdery mildew genomes (Fig. S1). Because RPW8.2 associates with the RING of GcR8IP1, we speculate that RPW8.2 may also interact with GcR8IP1 homologs in other PM fungi. This may partially explain why RPW8.2 confers broad-spectrum resistance to all tested infectious PM fungi (Xiao *et al.*, 2001). However, the role of GcR8IP1-RPW8.2 interaction in immunity is mechanistically distinct from that of the conventional Avr-R recognition in ETI against PM, such as the MLA-AVR_A recognition in barley-PM and Pms-AvrPms in wheat-PM interactions (Bourras *et al.*, 2019; Saur *et al.*, 2019; Bettgenhaeuser *et al.*, 2021). First, RPW8.2 may function as an executor rather than an immune receptor to recognize GcR8IP1 and initiate defense signaling. RPW8.2 seems to be passively hijacked by GcR8IP1 to localise to the nucleus where its accumulation triggers a SA-dependent self-amplification, leading to defense activation (Fig. 7). Second, the molecular warfare during canonical ETI is featured with a rapid HR within hours in the cases of bacteria, or 2 days with fungi and the interacted R-Avr triggers cell death when they are transiently co-expressed (Bourras *et al.*, 2019; Saur *et al.*, 2019; Bettgenhaeuser *et al.*, 2021; Sun *et al.*, 2021), whereas PM-induced RPW8-mediated HR occurs at 3 dpi or later (Xiao *et al.*, 2003; Wang *et al.*, 2009). This is consistent with our data that GcR8IP1 obviously suppresses RPW8.2-mediated immunity in both transient and stable expression assays in early infection stages when

RPW8.2 protein expression level is rather low (Fig. 5c and Fig. S7, S8). However, when RPW8.2 gets amplified above a threshold level through GcR8IP1-promoted nuclear localisation and accumulation, RPW8.2-mediated defense not only offsets GcR8IP1-mediated immunosuppression, but also greatly stimulates EDS1- and SA-dependent signaling to trigger HR and restrict fungal sporulation at day 3 and afterward (Fig. 5d and Fig. S7b, S9). Thus, the molecular interplay between GcR8IP1 and RPW8.2 is quite complicated, and its outcome depends on the basal level of SA-dependent defense, which determines the initial expression level of RPW8.2, and the level of GcR8IP1, which is probably determined by the quantity and activity of PM haustoria in the invaded host cells. Such a complex interplay offers a plausible new explanation for PM-induced and RPW8.2 dosage-dependent broad-spectrum resistance against PM fungi.

Acknowledgements

We thank S. Somerville for the *G. cichoracearum* UCSC1 isolate and F. Katagiri for the *pad4-1 sid2-1* mutant. This work was partially supported by the National Natural Science Foundation of China (No. U19A2033 to W-M.W. and 32121003 to X-W.C.), the Sichuan Youth Science and Technology Innovation Research Team Foundation (2022JDTD0023 to J.F.), the Natural Science Foundation of Sichuan Province (2022NSFSC0174 to H.W. and 2022NSFSC1699 to Z-X.Z.), and the National Science Foundation (No. IOS-1457033 and IOS-1901566 to S.X.).

Author contributions

W.-M.W., J.-H.Z., S.X., X.-J.W., and X.-W.C. designed experiments and analyzed data; J.-H.Z., Z.-X.Z., and Y.-Y.H. generated and characterized genetic material; J.-H.Z., Y.L., and Z-X.Z. performed cell death and pathogen growth assays; J.-H.Z., J.F., Y.-Y.H., S.-X.Z., G.-B.L. contributed to immunoprecipitation and immunofluorescence analyses; J.-H.Z., X.-M.Y., H.W., M.P., B.H., X.-H.H. and J.-W.Z. designed and performed protein-protein interaction assays in yeast and *N. benthamiana*. J.-H.Z., W.-M.W., S.X., J.F. and X.-J.W. wrote the manuscript with contributions from all authors.

Competing interests

None declared.

ORCID

Jing-Hao Zhao https://orcid.org/0000-0002-1347-3056
Shun-yuan Xiao https://orcid.org/0000-0003-1348-4879
Xian-Jun Wu https://orcid.org/0000-0003-0157-0235
Jing Fan https://orcid.org/0000-0002-6747-4302
Wen-Ming Wang https://orcid.org/0000-0002-6652-5964
Xiao-Hong Hu https://orcid.org/0000-0003-3104-0876
Yan-Yan Huang https://orcid.org/0000-0001-7688-0997
Guo-Bang Li https://orcid.org/0000-0001-5333-9321
Yan Li https://orcid.org/0000-0002-6443-9245
He Wang https://orcid.org/0000-0001-9654-6283
Xue-Mei Yang https://orcid.org/0000-0002-2546-5723
Ji-Wei Zhang https://orcid.org/0000-0001-7402-4089
Zhi-Xue Zhao https://orcid.org/0000-0002-3450-8422
Shi-Xin Zhou https://orcid.org/0000-0001-8055-3569

Data availability

The data that support the findings of this study are available from the corresponding authors upon reasonable request.

References

Bendtsen JD, Jensen LJ, Blom N, Von Heijne G, Brunak S. 2004. Feature-based prediction of non-classical and leaderless protein secretion. *Protein Engineering, Design and Selection* **17**: 349–356.

Bernoux M, Timmers T, Jauneau A, Brière C, De Wit PJGM, Marco Y, Deslandesa L. 2008. RD19, an *Arabidopsis* cysteine protease required for RRS1-R-mediated resistance, is relocalized to the nucleus by the *Ralstonia solanacearum* PopP2 effector. *Plant Cell* **20**: 2252–2264.

Bettgenhaeuser J, Hernández-Pinzón I, Dawson AM, Gardiner M, Green P, Taylor J, Smoker M, Ferguson JN, Emmrich P, Hubbard A, *et al.* 2021. The barley immune receptor Mla recognizes multiple pathogens and contributes to host

range dynamics. *Nature Communications* **12**: 1–14.

Bi G, Su M, Li N, Liang Y, Dang S, Xu J, Hu M, Wang J, Zou M, Deng Y, *et al.* 2021. The ZAR1 resistosome is a calcium-permeable channel triggering plant immune signaling. *Cell* **184**: 3528-3541.e12.

Bourras S, Kunz L, Xue M, Praz CR, Müller MC, Kälin C, Schläfli M, Ackermann P, Flückiger S, Parlange F, *et al.* 2019. The AvrPm3-Pm3 effector-NLR interactions control both race-specific resistance and host-specificity of cereal mildews on wheat. *Nature Communications* **10**: 1–16.

Brundrett MC, Enstone DE, Peterson CA. 1988. A berberine-aniline blue fluorescent staining procedure for suberin, lignin, and callose in plant tissue. *Protoplasma* **146**: 133–142.

Busso D, Keriel A, Sandrock B, Poterszman A, Gileadi O, Egly JM. 2000. Distinct regions of MAT1 regulate cdk7 kinase and TFIIH transcription activities. *Journal of Biological Chemistry* **275**: 22815–22823.

Butler WL, Kitajima M. 1975. Energy transfer between photosystem II and photosystem I in chloroplasts. *BBA - Bioenergetics* **396**: 72–85.

Castel B, Ngou PM, Cevik V, Redkar A, Kim DS, Yang Y, Ding P, Jones JDG. 2019. Diverse NLR immune receptors activate defence via the RPW8-NLR NRG1. *New Phytologist* **222**: 966–980.

Chang C, Yu D, Jiao J, Jing S, Schulze-Lefert P, Shen QH. 2013. Barley MLA immune receptors directly interfere with antagonistically acting transcription factors to initiate disease resistance signaling. *Plant Cell* **25**: 1158–1173.

Chen X, Duan Y, Qiao F, Liu H, Huang J, Luo C, Chen X, Li G, Xie K, Hsiang T, *et al.* 2022. A secreted fungal effector suppresses rice immunity through host histone hypoacetylation. *New Phytologist* **235**: 1977–1994.

Chen H, Zou Y, Shang Y, Lin H, Wang Y, Cai R, Tang X, Zhou JM. 2008. Firefly luciferase complementation imaging assay for protein-protein interactions in plants. *Plant Physiology* **146**: 368–376.

Clough SJ, Bent AF. 1998. Floral dip: A simplified method for Agrobacterium-mediated transformation of *Arabidopsis thaliana*. *Plant Journal* **16**: 735–743.

Collier SM, Hamel LP, Moffett P. 2011. Cell death mediated by the N-terminal domains of a unique and highly conserved class of NB-LRR protein. *Molecular Plant-Microbe Interactions* **24**: 918–931.

Dong OX, Tong M, Bonardi V, El Kasmi F, Woloshen V, Wünsch LK, Dangl JL, Li X. 2016. TNL-mediated immunity in Arabidopsis requires complex regulation of the redundant ADR1 gene family. *New Phytologist* **210**: 960–973.

Feaver WJ, Henry NL, Wang Z, Wu X, Svejstrup JQ, Bushnell DA, Friedberg EC, Kornberg RD. 1997. Genes for Tfb2, Tfb3, and Tfb4 subunits of yeast transcription/repair factor IIH: Homology to human cyclin-dependent kinase activating kinase and iih subunits. *Journal of Biological Chemistry* **272**: 19319–19327.

Horsefield S, Burdett H, Zhang X, Manik MK, Shi Y, Chen J, Qi T, Gilley J, Lai JS, Rank MX, *et al.* 2019. NAD^+ cleavage activity by animal and plant TIR domains in cell death pathways. *Science* **365**: 793–799.

Huang YY, Shi Y, Lei Y, Li Y, Fan J, Xu YJ, Ma XF, Zhao JQ, Xiao S, Wang WM. 2014. Functional identification of multiple nucleocytoplasmic trafficking signals in the broad-spectrum resistance protein RPW8.2. *Planta* **239**: 455–468.

Huang YY, Zhang LL, Ma XF, Zhao ZX, Zhao JHQ, Zhao JHQ, Fan J, Li Y, He P, Xiao S, *et al.* 2019. Multiple intramolecular trafficking signals in RESISTANCE TO POWDERY MILDEW 8.2 are engaged in activation of cell death and defense. *Plant Journal* **98**: 55–70.

Hückelhoven R, Panstruga R. 2011. Cell biology of the plant-powdery mildew interaction. *Current Opinion in Plant Biology* **14**: 738–746.

Jacobs KA, Collins-Racie LA, Colbert M, Duckett M, Golden-Fleet M, Kelleher K, Kriz R, LaVallie ER, Merberg D, Spaulding V, *et al.* 1997. A genetic selection for isolating cDNAs encoding secreted proteins. *Gene* **198**: 289–296.

Jones JDG, Dangl JL. 2006. The plant immune system. *Nature* **444**: 323–329.

Kim H, O'Connell R, Maekawa-Yoshikawa M, Uemura T, Neumann U, Schulze-Lefert P. 2014. The powdery mildew resistance protein RPW8.2 is carried on VAMP721/722 vesicles to the extrahaustorial membrane of haustorial complexes.

Plant Journal **79**: 835–847.

Koh S, André A, Edwards H, Ehrhardt D, Somerville S. 2005. *Arabidopsis thaliana* subcellular responses to compatible Erysiphe cichoracearum infections. *Plant Journal* **44**: 516–529.

Kourelis J, Van Der Hoorn RAL. 2018. Defended to the nines: 25 years of resistance gene cloning identifies nine mechanisms for R protein function. *Plant Cell* **30**: 285–299.

Kuckenberg J, Tartachnyk I, Noga G. 2009. Temporal and spatial changes of chlorophyll fluorescence as a basis for early and precise detection of leaf rust and powdery mildew infections in wheat leaves. *Precision Agriculture* **10**: 34–44.

Kwaaitaal M, Nielsen ME, Böhlenius H, Thordal-Christensen H. 2017. The plant membrane surrounding powdery mildew haustoria shares properties with the endoplasmic reticulum membrane. *Journal of Experimental Botany* **68**: 5731–5743.

Leclercq J, Lardet L, Martin F, Chapuset T, Oliver G, Montoro P. 2010. The green fluorescent protein as an efficient selection marker for *Agrobacterium tumefaciens*-mediated transformation in *Hevea brasiliensis* (Müll. Arg). *Plant Cell Reports* **29**: 513–522.

Li GB, Fan J, Wu JL, He JX, Liu J, Shen S, Gishkori ZGN, Hu XH, Zhu Y, Zhou SX, *et al.* 2021. The Flower-Infecting Fungus *Ustilaginoidea virens* Subverts Plant Immunity by Secreting a Chitin-Binding Protein. *Frontiers in Plant Science* **12**: 1–12.

Li H, Wang H, Jing M, Zhu J, Guo B, Wang Y, Lin Y, Chen H, Kong L, Ma Z, *et al.* 2018. A phytophthora effector recruits a host cytoplasmic transacetylase into nuclear speckles to enhance plant susceptibility. *eLife* **7**: 1–23.

Li Y, Zhang QQ, Zhang J, Wu L, Qi Y, Zhou JM. 2010. Identification of microRNAs involved in pathogen-associated molecular pattern-triggered plant innate immunity. *Plant Physiology* **152**: 2222–2231.

Lipka U, Fuchs R, Lipka V. 2008. *Arabidopsis* non-host resistance to powdery mildews. *Current Opinion in Plant Biology* **11**: 404–411.

Luo Q, Lian HL, He SB, Li L, Jia KP, Yang HQ. 2014. COP1 and phyB physically interact with PIL1 to regulate its stability and photomorphogenic development in Arabidopsis. *Plant Cell* **26**: 2441–2456.

Ma XF, Li Y, Sun JL, Wang TT, Fan J, Lei Y, Huang YY, Xu YJ, Zhao JQ, Xiao S, *et al.* 2014. Ectopic expression of RESISTANCE to POWDERY MILDEW8.1 confers resistance to fungal and oomycete pathogens in *Arabidopsis*. *Plant and Cell Physiology* **55**: 1484–1496.

Mason KN, Ekanayake G, Heese A. 2020. Staining and automated image quantification of callose in *Arabidopsis* cotyledons and leaves. In: Methods in Cell Biology. Elsevier Inc., 181–199.

Micali C, Göllner K, Humphry M, Consonni C, Panstruga R. 2008. The powdery mildew disease of *Arabidopsis*: a paradigm for the interaction between plants and biotrophic fungi. *The Arabidopsis Book* **6**: e0115.

Ngou BPM, Ahn HK, Ding P, Jones JDG. 2021. Mutual potentiation of plant immunity by cell-surface and intracellular receptors. *Nature* **592**: 110–115.

Nowara D, Schweizer P, Gay A, Lacomme C, Shaw J, Ridout C, Douchkov D, Hensel G, Kumlehn J. 2010. HIGS: Host-induced gene silencing in the obligate biotrophic fungal pathogen *Blumeria graminis*. *Plant Cell* **22**: 3130–3141.

Orgil U, Araki H, Tangchaiburana S, Berkey R, Xiao S. 2007. Intraspecific genetic variations, fitness cost and benefit of RPW8, a disease resistance locus in *Arabidopsis thaliana*. *Genetics* **176**: 2317–2333.

Peart JR, Mestre P, Lu R, Malcuit I, Baulcombe DC. 2005. NRG1, a CC-NB-LRR protein, together with N, a TIR-NB-LRR protein, mediates resistance against tobacco mosaic virus. *Current Biology* **15**: 968–973.

Roberts M, Tang S, Stallmann A, Dangl JL, Bonardi V. 2013. Genetic requirements for signaling from an autoactive plant NB-LRR intracellular innate immune receptor. *PLoS Genetics* **9**.

Saado I, Chia K-S, Betz R, Alcântara A, Pettkó-Szandtner A, Navarrete F, D'Auria JC, Kolomiets M V, Melzer M, Feussner I, *et al.* 2022. Effector-mediated relocalization of a maize lipoxygenase protein triggers susceptibility to

Ustilago maydis. *The Plant Cell* **34**: 2785–2805.

Saile SC, Jacob P, Castel B, Jubic LM, Salas-Gonzáles I, Bäcker M, Jones JDG, Dangl JL, El Kasmi F. 2020. Two unequally redundant 'helper' immune receptor families mediate Arabidopsis thaliana intracellular 'sensor' immune receptor functions. *PLoS biology* **18**: e3000783.

Saur IML, Bauer S, Kracher B, Lu X, Franzeskakis L, Müller MC, Sabelleck B, Kümmel F, Panstruga R, Maekawa T, *et al.* 2019. Multiple pairs of allelic MLA immune receptor-powdery mildew AVR a effectors argue for a direct recognition mechanism. *eLife* **8**: 1–31.

Schlücking K, Edel KH, Drerup MM, Köster P, Eckert C, Leonie S, Waadt R, Batistic O, Kudla J. 2013. A new β-estradiol-inducible vector set that facilitates easy construction and efficient expression of transgenes reveals CBL3-Dependent cytoplasm to tonoplast translocation of CIPK5. *Molecular Plant* **6**: 1814–1829.

Schultz P, Fribourg S, Poterszman A, Mallouh V, Moras D, Egly JM. 2000. Molecular structure of human TFIIH. *Cell* **102**: 599–607.

Von Stetten D, Noirclerc-Savoye M, Goedhart J, Gadella TWJ, Royant A. 2012. Structure of a fluorescent protein from Aequorea victoria bearing the obligate-monomer mutation A206K. *Acta Crystallographica Section F: Structural Biology and Crystallization Communications* **68**: 878–882.

Sun X, Lapin D, Feehan JM, Stolze SC, Kramer K, Dongus JA, Rzemieniewski J, Blanvillain-Baufumé S, Harzen A, Bautor J, *et al.* 2021. Pathogen effector recognition-dependent association of NRG1 with EDS1 and SAG101 in TNL receptor immunity. *Nature Communications* **12**: 1–15.

Teufel F, Almagro Armenteros JJ, Johansen AR, Gíslason MH, Pihl SI, Tsirigos KD, Winther O, Brunak S, von Heijne G, Nielsen H. 2022. SignalP 6.0 predicts all five types of signal peptides using protein language models. *Nature Biotechnology* **40**: 1023–1025.

Varsha Wesley S, Helliwell CA, Smith NA, Wang M, Rouse DT, Liu Q, Gooding PS, Singh SP, Abbott D, Stoutjesdijk PA, *et al.* 2001. Construct design for efficient, effective and high-throughput gene silencing in plants. *Plant Journal* **27**:

581–590.

Wan L, Essuman K, Anderson RG, Sasaki Y, Monteiro F, Chung EH, Nishimura EO, DiAntonio A, Milbrandt J, Dangl JL, *et al.* 2019. TIR domains of plant immune receptors are NAD^+-cleaving enzymes that promote cell death. *Science* **365**: 799–803.

Wang J, Hu M, Wang J, Qi J, Han Z, Wang G, Qi Y, Wang H-W, Zhou J-M, Chai J. 2019. Reconstitution and structure of a plant NLR resistosome conferring immunity. *Science* **364**: 44.

Wang W, Wen Y, Berkey R, Xiao S. 2009. Specific targeting of the *Arabidopsis* resistance protein RPW8.2 to the interfacial membrane encasing the fungal haustorium renders broad-spectrum resistance to powdery mildew. *Plant Cell* **21**: 2898–2913.

Wang W, Ye R, Xin Y, Fang X, Li C, Shi H, Zhou X, Qi Y. 2011. An importin β protein negatively regulates microRNA activity in *Arabidopsis*. *Plant Cell* **23**: 3565–3576.

Weßling R, Panstruga R. 2012. Rapid quantification of plant-powdery mildew interactions by qPCR and conidiospore counts. *Plant Methods* **8**.

Wu Z, Li M, Dong OX, Xia S, Liang W, Bao Y, Wasteneys G, Li X. 2019. Differential regulation of TNL-mediated immune signaling by redundant helper CNLs. *New Phytologist* **222**: 938–953.

Wydro M, Kozubek E, Lehmann P. 2006. Optimization of transient Agrobacterium-mediated gene expression system in leaves of *Nicotiana benthamiana*. *Acta Biochimica Polonica* **53**: 289–298.

Xiao S, Brown S, Patrick E, Brearley C, Turner JG. 2003. Enhanced transcription of the *Arabidopsis* disease resistance genes RPW8. 1 and RPW8. 2 via a salicylic acid-dependent amplification circuit is required for hypersensitive cell death. *Plant Cell* **15**: 33–45.

Xiao S, Calis O, Patrick E, Zhang G, Charoenwattana P, Muskett P, Parker JE, Turner JG. 2005. The atypical resistance gene, RPW8, recruits components of basal defence for powdery mildew resistance in *Arabidopsis*. *Plant Journal* **42**:

95–110.

Xiao S, Ellwood S, Calis O, Patrick E, Li T, Coleman M, Turner JG. 2001. Broad-spectrum mildew resistance in *Arabidopsis thaliana* mediated by RPW8. *Science* **291**: 118–120.

Xiao S, Emerson B, Ratanasut K, Patrick E, O'Neill C, Bancroft I, Turner JG. 2004. Origin and maintenance of a broad-spectrum disease resistance locus in *Arabidopsis*. *Molecular Biology and Evolution* **21**: 1661–1672.

Yu D, Song W, Tan EYJ, Liu L, Cao Y, Jirschitzka J, Li E, Logemann E, Xu C, Huang S, *et al.* 2022. TIR domains of plant immune receptors are 2′,3′-cAMP/cGMP synthetases mediating cell death. *Cell* **185**: 2370-2386.e18.

Yuan M, Jiang Z, Bi G, Nomura K, Liu M, Wang Y, Cai B, Zhou JM, He SY, Xin XF. 2021. Pattern-recognition receptors are required for NLR-mediated plant immunity. *Nature* **592**: 105–109.

Supporting Information

Figure legends

Fig. 1 RPW8.2 interacts with GcR8IP1.

(a) A schematic diagram shows GcR8IP1, RPW8.2, and their truncated versions. Numbers indicate amino acid positions. NT, the first 100 amino acid residues (aa) of RPW8.2. CT, the 101-174 aa of RPW8.2.

(b) Yeast two-hybrid (Y2H) assay for detecting the associations between RPW8.2, GcR8IP1, and their truncated versions. SD-LW indicates SD medium lacking Leu and Trp. SD-LWHA/AbA indicates SD lacking adenine, histidine, leucine, and tryptophan, but with AbA.

(c) Bimolecular fluorescence complementation (BiFC) assay shows the associations

between RPW8.2, GcR8IP1, and their truncated versions. YN-CIPK24 and YC-CBL10 were used as positive controls. YN-CIPK24 and YC-RPW8.2 were used as negative controls. 2RFP-NLS was used as a nucleus maker. Size bar, 10 μm.

(d) A semi-*in vitro* GST pull-down assay shows the interaction of RPW8.2-HA with GST-GcR8IP1-M1 (GST-M1). GST or GST-M1 immobilized on GST beads was co-incubated with lysates of *Nicotiana benthamiana* leaves transiently expressing *35S$_{pro}$:RPW8.2-HA*. The beads were washed and pelleted for immunoblotting with GST and HA antibodies. The input lysates of *35S$_{pro}$:RPW8.2-HA* were added as expression control (*).

(e) Co-immunoprecipitation assay shows the interaction of RPW8.2-FLAG with GcR8IP1-HA. Total proteins were extracted from *N. benthamiana* leaves co-expressing *35S$_{pro}$:RPW8.2-FLAG* with *35S$_{pro}$:GcR8IP1-HA* or *35S$_{pro}$:GcR8IP1-M2-HA* (M2-HA). Protein complexes were pulled down using agarose beads conjugated with an HA antibody and the co-precipitated complex was examined by Western blotting using FLAG and HA antibodies. The higher molecular bands (*) may indicate protein complex mediated by the full-length of GcR8IP1.

Fig. 2 GcR8IP1 is a secretory protein and translocated into the nucleus of host cell.

(a) Validation of the GcR8IP1 signal peptide by yeast invertase secretion assay. The DNA fragment encoding the first 16 aa, 26 aa or 40 aa of GcR8IP1 was in-frame fused to yeast mature invertase sequence in the pSUC2 vector and expressed in YTK12. The N-terminal sequence of Mg87 and the signal peptide of Avr1b were used as the negative and positive control, respectively.

(b) Validation of the GcR8IP1 signal peptide in *N. benthamiana*. Leaves transiently expressing the first 40 aa of GcR8IP1 fused with GFP (GcR8IP1-N40 aa-GFP) or GFP were stained with FM4-64 and imaged at 48 hpi under a confocal microscope. Note that GcR8IP1-N40 aa-GFP was secreted into the apoplast (arrows). Sucrose +: leaf discs were treated with 12% sucrose for 10 min to achieve plasmolysis. Size bars, 25 μm.

(c) Immunofluorescence staining images show the localisation of GcR8IP1 in the

nucleus (arrow). The slides were prepared from *Arabidopsis pad4-1 sid2-1* leaves at 3 days post inoculation of *G. cichoracearum* UCSC1. The subcellular localisation of GcR8IP1 (green) was detected by a primary antibody raised against GcR8IP1 and visualized by Alexa Fluor® 488-conjugated secondary antibody (AF488) that binds with the primary antibody. The nucleus (blue) was counterstained with 4',6-diamidino-2-phenylindole (DAPI). H: haustoria. α-R8IP1: antibody of GcR8IP1. Mock: rabbit antisera. Size bar, 10 μm.

Fig. 3 GcR8IP1 increases the partitioning of RPW8.2 in the nucleus.

(a) Representative confocal images show the subcellular localisation of the indicated proteins. *R82$_{pro}$:RPW8.2-GFP* was transiently co-expressed with *35S$_{pro}$:GcR8IP1-RFP* (upper panel) and *35S$_{pro}$:2RFP-NLS* (lower panel) in *N. benthamiana* leaves via agrobacteria-mediated infiltration and images were acquired at 48 hours post infiltration. Size bars, 50 μm.

(b) Frequency of cells with RPW8.2-GFP in the nucleus. At least 200 cells were counted (refer to Fig. S5).

(c, d) Magnified confocal images show the subcellular localisation of the RPW8.2-GFP when co-expressed with GcR8IP1-RFP (c) or 2RFP-NLS (d). Size bar, 20 μm.

(e, f) Scan line analysis of the fluorescence intensity of GFP and RFP at the position indicated by the lines in (c, d).

(g) Immunoblotting analysis on the partitioning of RPW8.2-HA in the nucleus and the cytoplasm when *35S$_{pro}$:RPW8.2-HA* was co-expressed with *35S$_{pro}$:2RFP-NLS* or *35S$_{pro}$:GcR8IP1* in *N. benthamiana*. H3 and PEPC is a nuclear and a cytoplasmic marker, respectively.

(h) A schematic diagram shows the nuclear localisation sequence and the sequence mutations in RPW8.2 and GcR8IP1.

(i) Representative confocal images show the subcellular localisation of the indicated proteins. The wild type *35S$_{pro}$:RPW8.2-GFP* or *35S$_{pro}$:RPW8.2^{nls}-GFP* mutant was co-

expressed with *35S$_{pro}$:GcR8IP1-RFP* or *35S$_{pro}$:GcR8IP1^{nls}-RFP* in *N. benthamiana* leaves via agrobacteria-mediated infiltration. Images were acquired at 48 hours post infiltration. Images are representative Z-stack projections of 17-26 optical sections. The numbers in white indicate the numbers of cells with nucleus-localised RPW8.2-GFP versus the numbers of cells expressing RPW8.2-GFP. Three independent leaf samples and 30-50 cells from each leaf sample were examined. Size bars, 50 μm.

Fig. 4 GcR8IP1 increases RPW8.2 accumulation.

(a) Dual-luciferase assay shows the relative luciferase activities of firefly luciferase versus renilla luciferase. Firefly luciferase was expressed from the *RPW8.2* promoter (*R82$_{pro}$:Luc*) and co-expressed with empty vector (EV), *35S$_{pro}$:RPW8.2*, *35S$_{pro}$:RPW8.2-NLS$_{Sv40}$*, *35S$_{pro}$:RPW8.2-nls$_{Sv40}$* and *35S$_{pro}$:RPW8.2-NES$_{PKI}$*, respectively. *35S$_{pro}$:Renilla luciferase* was used as the internal control. The data are shown as mean ± s.d. (n = 4 biological replicates×4 technical replicates). Different letters indicate significant differences ($P < 0.05$) as determined by the one-way Tukey–Kramer test.

(b) Representative confocal images of RPW8.2-YFP (*R82$_{pro}$:R82Y*) co-expressed with RPW8.2-HA (*35S$_{pro}$:R82HA*) plus GcR8IP1 or with RPW8.2-HA (*35S$_{pro}$:R82HA*) in *N. benthamiana*.

(c) Immunoblotting analysis of (b) shows protein abundance of RPW8.2-YFP. Total proteins from whole cells were isolated for analysis. The band intensity in the panel of α-GFP was normalized to that of Ponceau S panel for each sample, resulting in relative band intensity. Then, the relative band intensity was normalized to that of the control sample, which was set to 1. Data from three independent experiments are presented in a bar graph (n = 3 experimental replicates). Asterisks (**) denote significant difference ($P = 0.0035$), as determined by Student's *t*-test.

(d) Dual-luciferase assay shows the relative luciferase activities of firefly luciferase versus renilla luciferase. Data are shown as mean ± s.d. (n = 8 biological replicates × 6 technical replicates). Significance of difference was determined by Student's *t*-test.

****, $P < 0.0001$; ns, not significant.

(e) Immunoblotting analysis of the RPW8.2-YFP abundance when it was co-expressed with the indicated proteins. Total proteins from whole cells were isolated for analysis. Relative RPW8.2-YFP abundance was calculated by dividing the band intensity in the α-GFP panel by that in the Ponceau S panel for each sample. Relative RPW8.2-YFP abundance in the lane *$35S_{pro}$:RPW8.2-YFP + RPW8.2-HA* was used as the control. Data from three independent experiments are presented in a bar graph (n = 3 experimental replicates). Significance of difference was determined by Student's *t*-test. *, $P < 0.05$; ***, $P < 0.001$; ns, not significant.

Fig. 5 The molecular warfare engaged by GcR8IP1 and RPW8.2 at the infection site.

(a) Chlorophyll auto-fluorescence images of the wild-type Wa-1 and XVE-*GcR8IP1*-HA-OE transgenic lines at 10 days post inoculation (dpi) of *G. cichoracearum* UCSC1. Plants were sprayed with β-estradiol or DMSO (Mock) 12 h prior to UCSC1 inoculation.

(b) Quantification analysis of the chlorophyll fluorescence Fv/Fm from the indicated lines. The data are shown as mean ± s.d. (n = 3 biological replicates). Significance of difference was determined by Student's *t*-test. **, $P < 0.01$; ***, $P < 0.001$; ****, $P < 0.0001$; ns, not significant.

(c) Quantification of powdery mildew (PM) biomass by qPCR in the indicated lines. Relative fungal biomass was calculated by the comparison between *G. cichoracearum GDSL-like lipase* gene and *A. thaliana Glyceraldehyde-3-phosphate dehydrogenase of plastid 2* gene (*GAPCP-2*) at 10 dpi of *G. cichoracearum* UCSC1. The data are shown as mean ± s.d. (n = 3 biological replicates). Significance of difference was determined by Student's *t*-test. ****, $P < 0.0001$; ns, not significant.

(d) Quantification analysis on the sporulation of PM from the indicated lines at 10 dpi. The data are shown as mean ± s.d. (n = 3 biological replicates), and ns indicates no significant difference as determined by Student's *t*-test. ns, not significant.

(e) Confocal images show the expression of YFP from the *RPW8.2* promoter in the

transgenic plants P2Y3' at 2 days post inoculation of *G. cichoracearum* UCSC1. H, haustorium. PI, propidium iodide. Size bars, 100 μm (upper) and 20 μm (lower).

Fig. 6 GcR8IP1 facilitates powdery mildew pathogenesis.

(a) Chlorophyll auto-fluorescence images of the wild-type Col-0 and XVE-*GcR8IP1*-HA-OE transgenic lines at 10 days post inoculation (dpi) of *G. cichoracearum* UCSC1. Plants were sprayed with β-estradiol or DMSO (Mock) 12 h prior to UCSC1 inoculation.

(b) Quantification analysis on the chlorophyll fluorescence parameter Fv/Fm from the indicated lines. The data are shown as mean ± s.d. (n = 3~5 biological replicates). Significance of difference was determined by Student's *t*-test. ****, $P < 0.0001$; ns, not significant.

(c) Quantification of relative PM biomass by qPCR in the indicated lines. Relative fungal biomass was calculated by the comparison between *G. cichoracearum GDSL-like lipase* gene and *A. thaliana Glyceraldehyde-3-phosphate dehydrogenase of plastid 2* gene (*GAPCP-2*) at 10 dpi of *Gc* UCSC1. The data are shown as mean ± s.d. (n = 3 biological replicates). Significance of difference was determined by Student's *t*-test. ****, $P < 0.0001$; ns, not significant.

(d) Quantification analysis on the sporulation of PM from the indicated lines at 10 dpi. The data are shown as mean ± s.d. (n = 3 biological replicates). Significance of difference was determined by Student's *t*-test. ***, $P < 0.001$; ****, $P < 0.0001$; ns, not significant.

(e) Relative expression of *GcR8IP1* in indicated lines at 6 dpi of *Gc* UCSC1. Interference small RNA was used to silence *GFP* (GFP-IR) or *GcR8IP1* (R8IP1-IR) in the *pad4-1 sid2-1* background. The data are shown as mean ± s.d. (n = 3 biological replicates), and different letters indicate significant differences ($P < 0.05$) as determined by the one-way Tukey–Kramer test.

(f) PM disease phenotypes of the indicated lines. Photos were taken at 6 dpi of *Gc* UCSC1.

(g) Quantification analysis on the sporulation of PM from the indicated lines at 6 dpi. The data are shown as mean ± s.d. (n = 3 biological replicates). Different letters indicate significant differences ($P < 0.05$) as determined by the one-way Tukey–Kramer test.

Fig. 7 A working model for GcR8IP1-induced transcriptional amplification of RPW8.2 to activate immunity against powdery mildew.

PM delivers GcR8IP1 into the host to suppress immunity, presumably via suppression of PTI. GcR8IP1 increases RPW8.2's nuclear partitioning. Nucleus-localised RPW8.2 activates defense and the increased nucleus-localisation further increases its expression via a SA-dependent transcriptional amplification, leading to broad-spectrum resistance to powdery mildew. CW, cell wall. EHM, extrahaustorial membrane. H, haustoria. PM, plasma membrane.

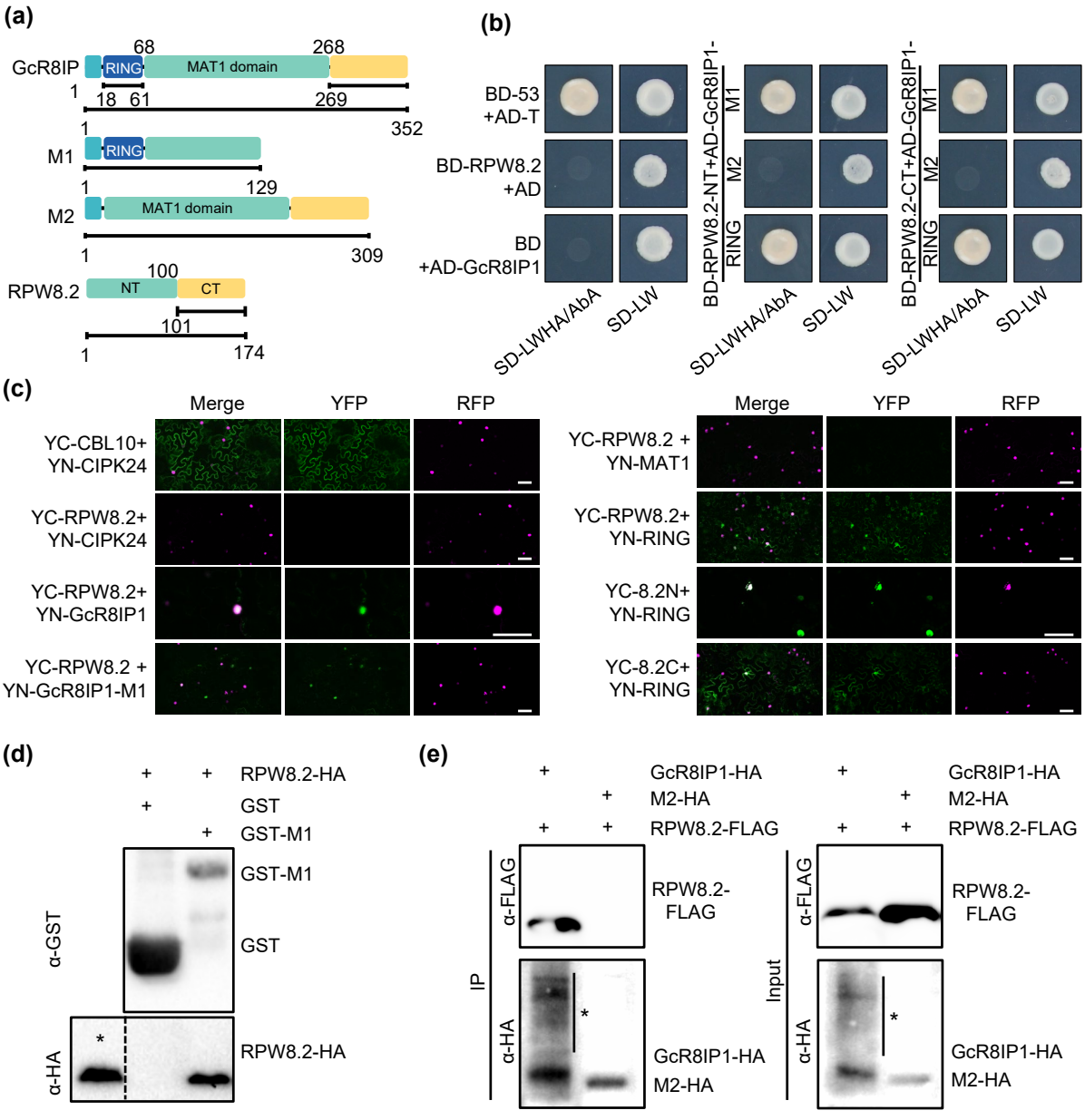

Fig. 1 RPW8.2 interacts with GcR8IP1.
(a) A schematic diagram shows GcR8IP1, RPW8.2, and their truncated versions. Numbers indicate amino acid positions. NT, the first 100 amino acid residues (aa) of RPW8.2. CT, the 101-174 aa of RPW8.2.
(b) Yeast two-hybrid (Y2H) assay for detecting the associations between RPW8.2, GcR8IP1, and their truncated versions. SD-LW indicates SD medium lacking Leu and Trp. SD-LWHA/AbA indicates SD lacking adenine, histidine, leucine, and tryptophan, but with AbA.
(c) Bimolecular fluorescence complementation (BiFC) assay shows the associations between RPW8.2, GcR8IP1, and their truncated versions. YN-CIPK24 and YC-CBL10 were used as positive controls. YN-CIPK24 and YC-RPW8.2 were used as negative controls. 2RFP-NLS was used as a nucleus maker. Size bar, 10 μm.
(d) A semi-*in vitro* GST pull-down assay shows the interaction of RPW8.2-HA with GST-GcR8IP1-M1 (GST-M1). GST or GST-M1 immobilized on GST beads was co-incubated with lysates of *Nicotiana benthamiana* leaves transiently expressing *$35S_{pro}$:RPW8.2-HA*. The beads were washed and pelleted for immunoblotting with GST and HA antibodies. The input lysates of 35Spro:RPW8.2-HA were added as expression control (*).
(e) Co-immunoprecipitation assay shows the interaction of RPW8.2-FLAG with GcR8IP1-HA. Total proteins were extracted from *N. benthamiana* leaves co-expressing *$35S_{pro}$:RPW8.2-FLAG* with *$35S_{pro}$:GcR8IP1-HA* or *$35S_{pro}$:GcR8IP1-M2-HA* (M2-HA). Protein complexes were pulled down using agarose beads conjugated with a HA antibody and the co-precipitated complex was examined by Western blotting using FLAG and HA antibodies. The higher molecular bands (*) may indicate protein complex mediated by the full-length of GcR8IP1.

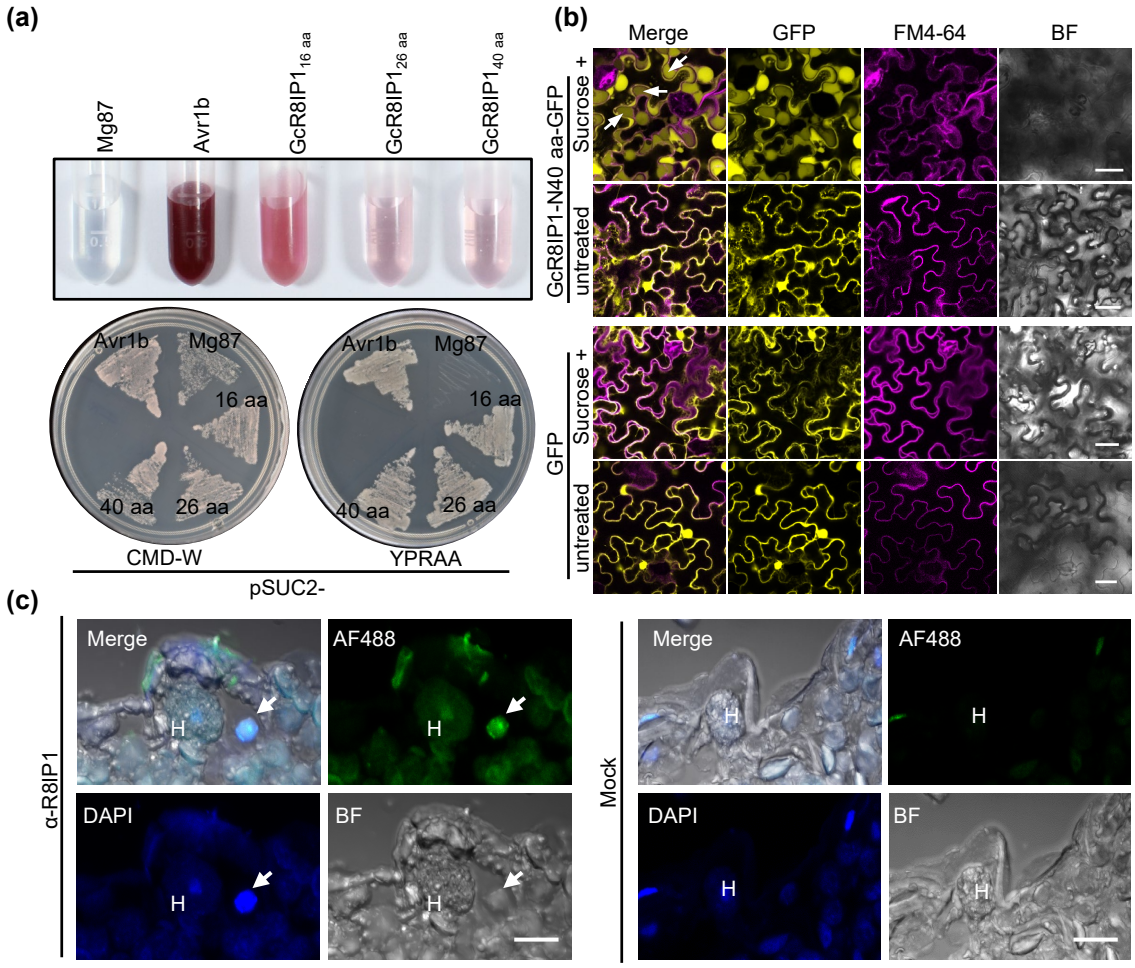

Fig. 2 GcR8IP1 is a secretory protein and translocated into the nucleus of host cell.
(a) Validation of the GcR8IP1 signal peptide by yeast invertase secretion assay. The DNA fragment encoding the first 16 aa, 26 aa or 40 aa of GcR8IP1 was in-frame fused to yeast mature invertase sequence in the pSUC2 vector and expressed in YTK12. The N-terminal sequence of Mg87 and the signal peptide of Avr1b were used as the negative and positive control, respectively.
(b) Validation of the GcR8IP1 signal peptide in *N. benthamiana*. Leaves transiently expressing the first 40 aa of GcR8IP1 fused with GFP (GcR8IP1-N40 aa-GFP) or GFP were stained with FM4-64 and imaged at 48 hpi under a confocal microscope. Note that GcR8IP1-N40 aa-GFP was secreted into the apoplast (arrows). Sucrose +: leaf discs were treated with 12% sucrose for 10 min to achieve plasmolysis. Size bars, 25 μm.
(c) Immunofluorescence staining images show the localisation of GcR8IP1 in the nucleus (arrow). The slides were prepared from *Arabidopsis pad4-1 sid2-1* leaves at 3 days post inoculation of *G. cichoracearum* UCSC1. The subcellular localisation of GcR8IP1 (green) was detected by a primary antibody raised against GcR8IP1 and visualized by Alexa Fluor® 488-conjugated secondary antibody (AF488) that binds with the primary antibody. The nucleus (blue) was counterstained with 4',6-diamidino-2-phenylindole (DAPI). H: haustoria. α-R8IP1: antibody of GcR8IP1. Mock: rabbit antisera. Size bar, 10 μm.

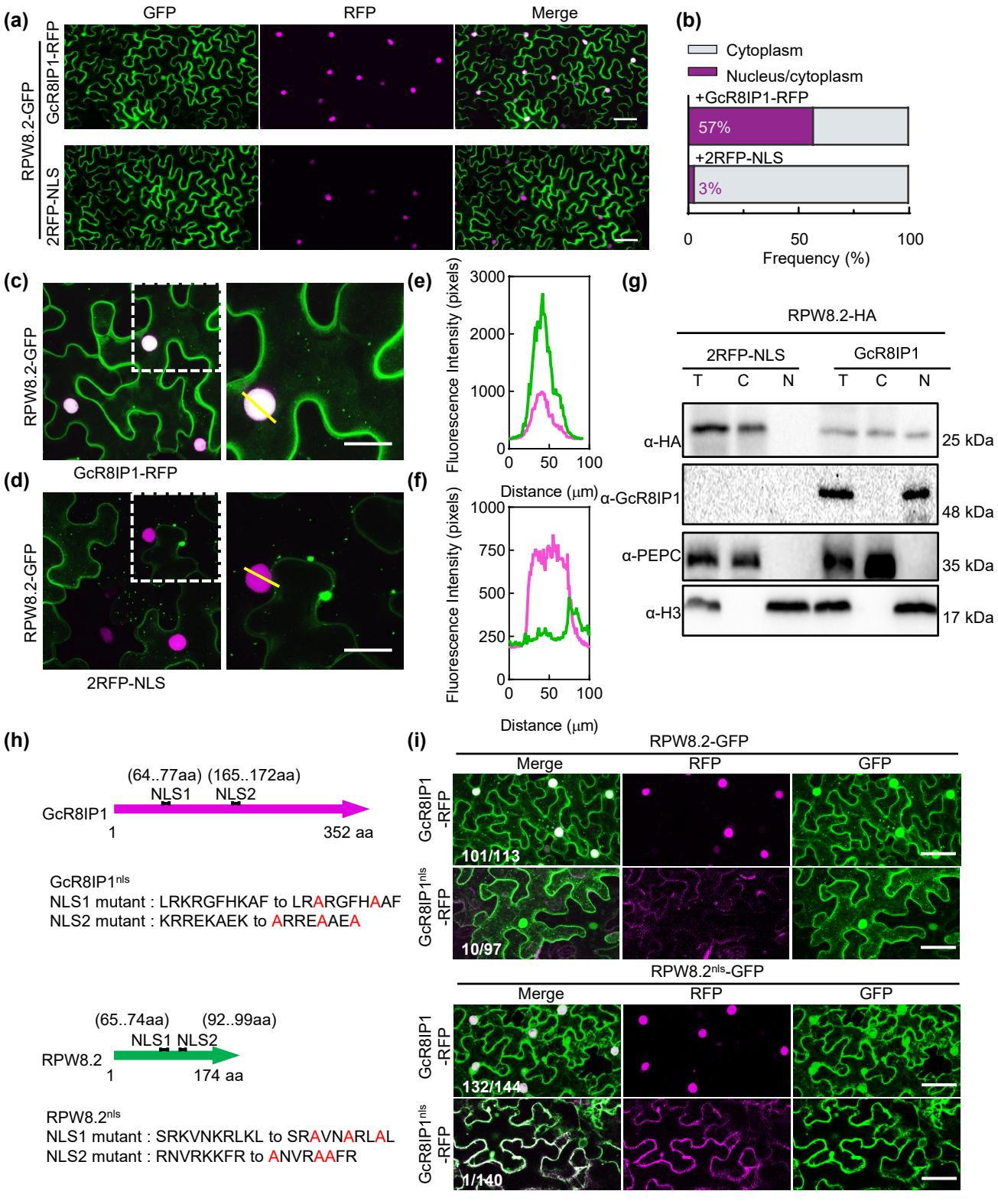

Fig. 3 GcR8IP1 increases the partitioning of RPW8.2 in the nucleus.

(a) Representative confocal images show the subcellular localisation of the indicated proteins. *R82$_{pro}$:RPW8.2-GFP* was transiently co-expressed with *35S$_{pro}$:GcR8IP1-RFP* (upper panel) and *35S$_{pro}$:2RFP-NLS* (lower panel) in *N. benthamiana* leaves via agrobacteria-mediated infiltration and images were acquired at 48 hours post infiltration. Size bars, 50 μm.

(b) Frequency of cells with RPW8.2-GFP in the nucleus. At least 200 cells were counted (refer to Fig. S5).

(c, d) Magnified confocal images show the subcellular localisation of the RPW8.2-GFP when co-expressed with GcR8IP1-RFP (c) or 2RFP-NLS (d). Size bar, 20 μm.

(e, f) Scan line analysis of the fluorescence intensity of GFP and RFP at the position indicated by the lines in (c, d).

(g) Immunoblotting analysis on the partitioning of RPW8.2-HA in the nucleus and the cytoplasm when *35S$_{pro}$:RPW8.2-HA* was co-expressed with *35S$_{pro}$:2RFP-NLS* or *35S$_{pro}$:GcR8IP1* in *N. benthamiana*. H3 and PEPC is a nuclear and a cytoplasmic marker, respectively.

(h) A schematic diagram shows the nuclear localisation sequence and the sequence mutations in RPW8.2 and GcR8IP1.

(i) Representative confocal images show the subcellular localisation of the indicated proteins. The wild type *35S$_{pro}$:RPW8.2-GFP* or *35S$_{pro}$:RPW8.2^{nls}-GFP* mutant was co-expressed with *35S$_{pro}$:GcR8IP1-RFP* or *35S$_{pro}$:GcR8IP1^{nls}-RFP* in *N. benthamiana* leaves via agrobacteria-mediated infiltration. Images were acquired at 48 hours post infiltration. Images are representative Z-stack projections of 17-26 optical sections. The numbers in white indicate the numbers of cells with nucleus-localised RPW8.2-GFP versus the numbers of cells expressing RPW8.2-GFP. Three independent leaf samples and 30-50 cells from each leaf sample were examined. Size bars, 50 μm.

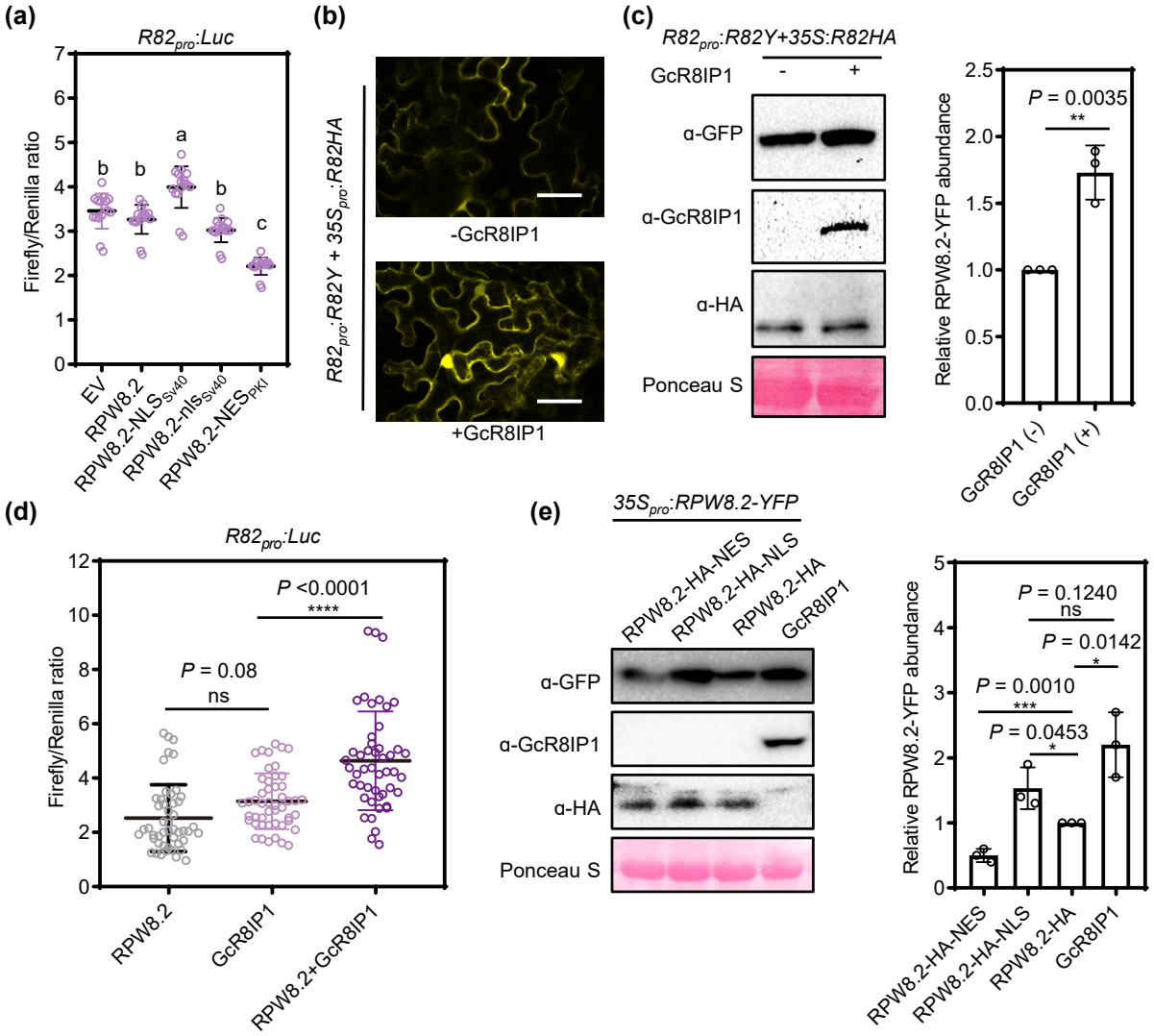

Fig. 4 GcR8IP1 increases RPW8.2 accumulation.

(a) Dual-luciferase assay shows the relative luciferase activities of firefly luciferase versus renilla luciferase. Firefly luciferase was expressed from the *RPW8.2* promoter ($R82_{pro}$*:Luc*) and co-expressed with empty vector (EV), $35S_{pro}$*:RPW8.2*, $35S_{pro}$*:RPW8.2-NLS*$_{Sv40}$, $35S_{pro}$*:RPW8.2-nls*$_{Sv40}$ and $35S_{pro}$*:RPW8.2-NES*$_{PKI}$, respectively. $35S_{pro}$*:Renilla luciferase* was used as the internal control. The data are shown as mean ± s.d. (n = 4 biological replicates × 4 technical replicates). Different letters indicate significant differences ($P < 0.05$) as determined by the one-way Tukey–Kramer test.

(b) Representative confocal images of RPW8.2-YFP ($R82_{pro}$*:R82Y*) co-expressed with RPW8.2-HA ($35S_{pro}$*:R82HA*) plus GcR8IP1 or with RPW8.2-HA ($35S_{pro}$*:R82HA*) in *N. benthamiana*.

(c) Immunoblotting analysis of (b) shows protein abundance of RPW8.2-YFP. Total proteins from whole cells were isolated for analysis. The band intensity in the panel of α-GFP was normalized to that of Ponceau S panel for each sample, resulting in relative band intensity. Then, the relative band intensity was normalized to that of the control sample, which was set to 1. Data from three independent experiments are presented in a bar graph (n = 3 experimental replicates). Asterisks (**) denote significant difference ($P = 0.0035$), as determined by Student's *t*-test.

(d) Dual-luciferase assay shows the relative luciferase activities of firefly luciferase versus renilla luciferase. Data are shown as mean ± s.d. (n = 8 biological replicates × 6 technical replicates). Significance of difference was determined by Student's *t*-test. ****, $P < 0.0001$; ns, not significant.

(e) Immunoblotting analysis of the RPW8.2-YFP abundance when it was co-expressed with the indicated proteins. Total proteins from whole cells were isolated for analysis. Relative RPW8.2-YFP abundance was calculated by dividing the band intensity in the α-GFP panel by that in the Ponceau S panel for each sample. Relative RPW8.2-YFP abundance in the lane $35S_{pro}$*:RPW8.2-YFP + RPW8.2-HA* was used as the control. Data from three independent experiments are presented in a bar graph (n = 3 experimental replicates). Significance of difference was determined by Student's *t*-test. *, $P < 0.05$; ***, $P < 0.001$; ns, not significant.

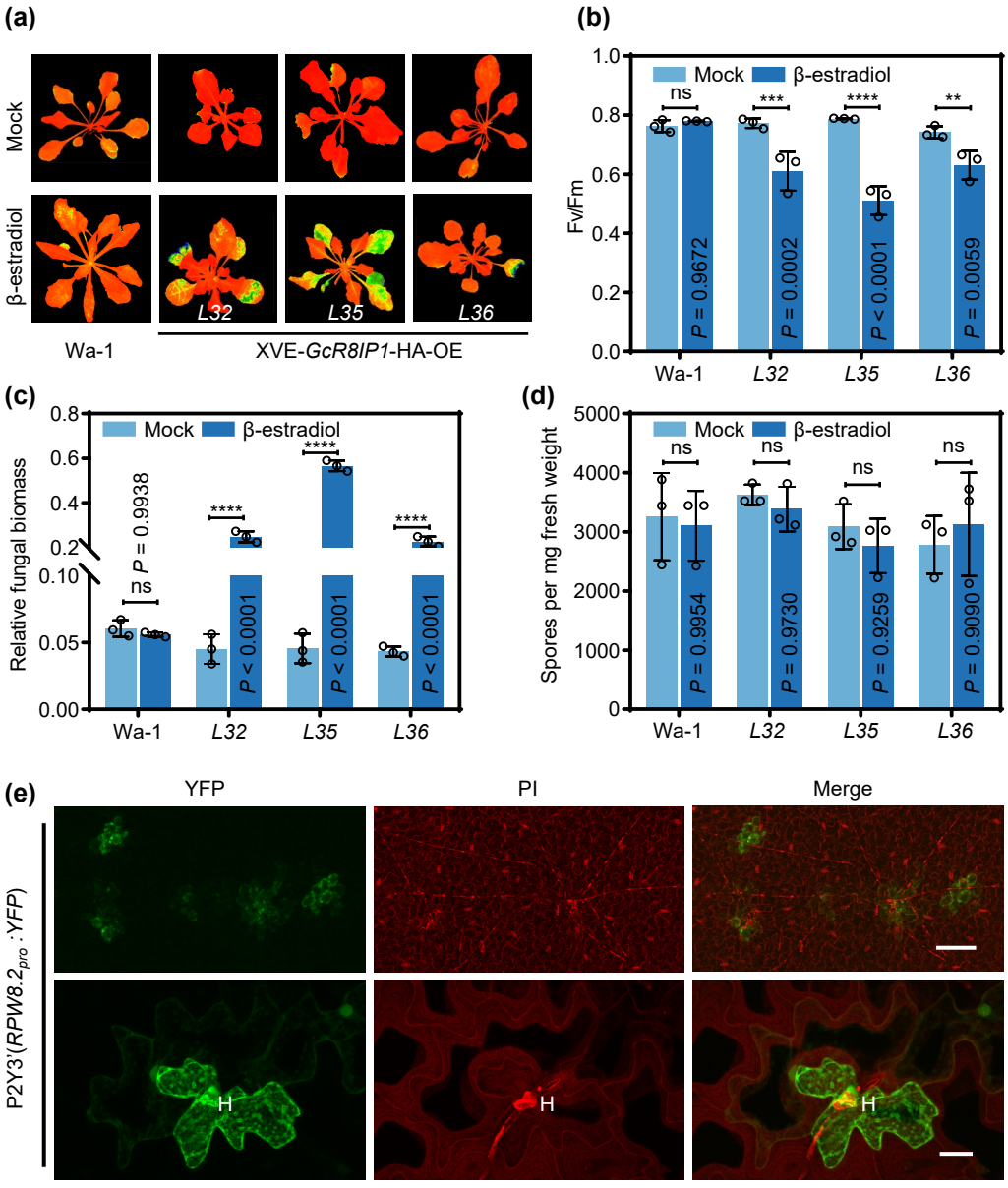

Fig. 5 The molecular warfare engaged by GcR8IP1 and RPW8.2 at the infection site.
(a) Chlorophyll auto-fluorescence images of the wild-type Wa-1 and XVE-*GcR8IP1*-HA-OE transgenic lines at 10 days post inoculation (dpi) of *G. cichoracearum* UCSC1. Plants were sprayed with β-estradiol or DMSO (Mock) 12 h prior to UCSC1 inoculation.
(b) Quantification analysis of the chlorophyll fluorescence Fv/Fm from the indicated lines. The data are shown as mean ± s.d. (n = 3 biological replicates). Significance of difference was determined by Student's *t*-test. **, $P < 0.01$; ***, $P < 0.001$; ****, $P < 0.0001$; ns, not significant.
(c) Quantification of powdery mildew (PM) biomass by qPCR in the indicated lines. Relative fungal biomass was calculated by the comparison between *G. cichoracearum GDSL-like lipase* gene and *A. thaliana Glyceraldehyde-3-phosphate dehydrogenase of plastid 2* gene (*GAPCP-2*) at 10 dpi of *G. cichoracearum* UCSC1. The data are shown as mean ± s.d. (n = 3 biological replicates). Significance of difference was determined by Student's *t*-test. ****, $P < 0.0001$; ns, not significant.
(d) Quantification analysis on the sporulation of PM from the indicated lines at 10 dpi. The data are shown as mean ± s.d. (n = 3 biological replicates), and ns indicates no significant difference as determined by Student's *t*-test. ns, not significant.
(e) Confocal images show the expression of YFP from the *RPW8.2* promoter in the transgenic plants P2Y3' at 2 days post inoculation of *G. cichoracearum* UCSC1. H, haustorium. PI, propidium iodide. Size bars, 100 μm (upper) and 20 μm (lower).

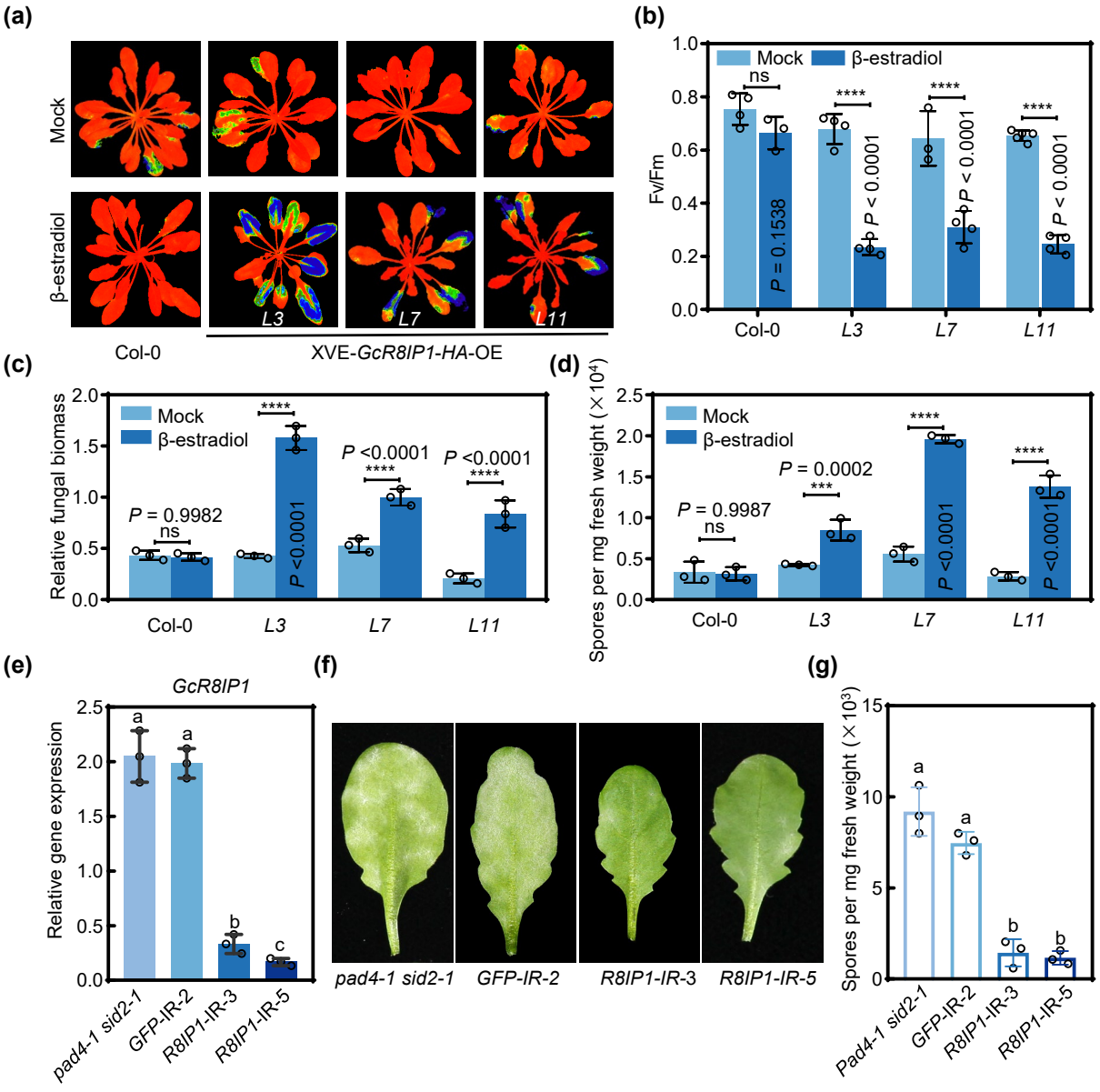

Fig. 6 GcR8IP1 facilitates powdery mildew pathogenesis.
(a) Chlorophyll auto-fluorescence images of the wild-type Col-0 and XVE-*GcR8IP1*-HA-OE transgenic lines at 10 days post inoculation (dpi) of *G. cichoracearum* UCSC1. Plants were sprayed with β-estradiol or DMSO (Mock) 12 h prior to UCSC1 inoculation.
(b) Quantification analysis on the chlorophyll fluorescence parameter Fv/Fm from the indicated lines. The data are shown as mean ± s.d. (n = 3 biological replicates). Significance of difference was determined by Student's *t*-test. ****, $P < 0.0001$; ns, not significant.
(c) Quantification of relative PM biomass by qPCR in the indicated lines. Relative fungal biomass was calculated by the comparison between *G. cichoracearum GDSL-like lipase* gene and *A. thaliana Glyceraldehyde-3-phosphate dehydrogenase of plastid 2* gene (*GAPCP-2*) at 10 dpi of *Gc* UCSC1. The data are shown as mean ± s.d. (n = 3 biological replicates). Significance of difference was determined by Student's *t*-test. ****, $P < 0.0001$; ns, not significant.
(d) Quantification analysis on the sporulation of PM from the indicated lines at 10 dpi. The data are shown as mean ± s.d. (n = 6 biological replicates). Significance of difference was determined by Student's *t*-test. ***, $P < 0.001$; ****, $P < 0.0001$; ns, not significant.
(e) Relative expression of *GcR8IP1* in indicated lines at 6 dpi of *Gc* UCSC1. Interference small RNA was used to silence *GFP* (GFP-IR) or *GcR8IP1* (R8IP1-IR) in the *pad4-1 sid2-1* background. The data are shown as mean ± s.d. (n = 3 biological replicates), and different letters indicate significant differences ($P < 0.05$) as determined by the one-way Tukey–Kramer test.
(f) PM disease phenotypes of the indicated lines. Photos were taken at 6 dpi of *Gc* UCSC1.
(g) Quantification analysis on the sporulation of PM from the indicated lines at 6 dpi. The data are shown as mean ± s.d. (n = 3 biological replicates). Different letters indicate significant differences ($P < 0.05$) as determined by the one-way Tukey–Kramer test.

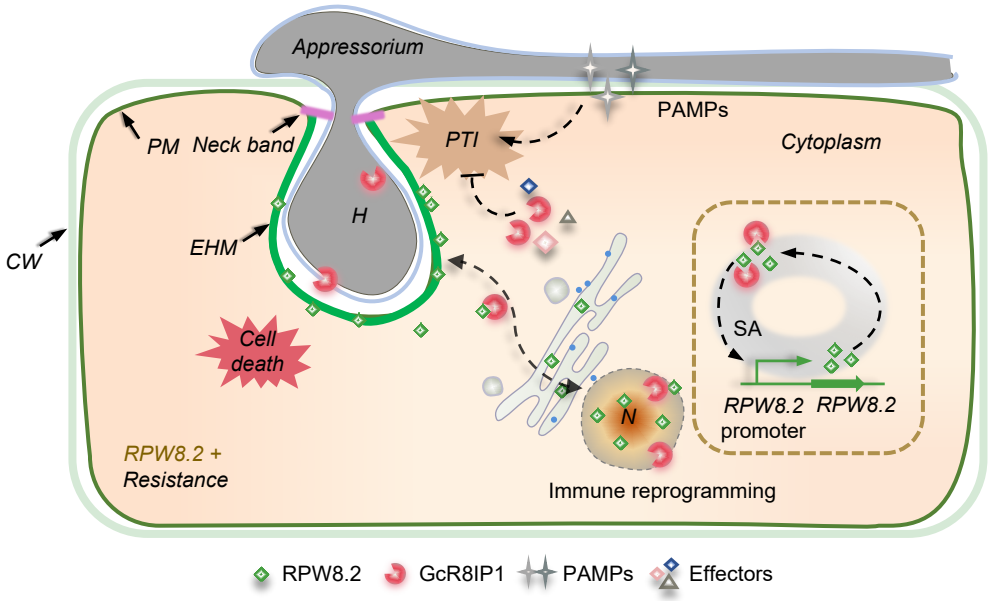

Fig. 7 A working model for GcR8IP1-induced transcriptional amplification of RPW8.2 to activate immunity against powdery mildew.
PM delivers GcR8IP1 into the host to suppress immunity, presumably via suppression of PTI. GcR8IP1 increases RPW8.2's nuclear partitioning. Nucleus-localised RPW8.2 activates defense and the increased nucleus-localisation further increases its expression via a SA-dependent transcriptional amplification, leading to broad-spectrum resistance to powdery mildew. CW, cell wall. EHM, extrahaustorial membrane. H, haustoria. PM, plasma membrane.